



National Library
of Canada

Bibliothèque nationale
du Canada

Canadian Theses Service Service des thèses canadiennes

Ottawa, Canada
K1A 0N4

NOTICE

The quality of this microform is heavily dependent upon the quality of the original thesis submitted for microfilming. Every effort has been made to ensure the highest quality of reproduction possible.

If pages are missing, contact the university which granted the degree.

Some pages may have indistinct print especially if the original pages were typed with a poor typewriter ribbon or if the university sent us an inferior photocopy.

Previously copyrighted materials (journal articles, published tests, etc.) are not filmed.

Reproduction in full or in part of this microform is governed by the Canadian Copyright Act; R.S.C. 1970, c. C-30.

AVIS

La qualité de cette microforme dépend grandement de la qualité de la thèse soumise au microfilmage. Nous avons tout fait pour assurer une qualité supérieure de reproduction.

S'il manque des pages, veuillez communiquer avec l'université qui a conféré le grade.

La qualité d'impression de certaines pages peut laisser à désirer, surtout si les pages originales ont été dactylographiées à l'aide d'un ruban usé ou si l'université nous a fait parvenir une photocopie de qualité inférieure.

Les documents, qui font déjà l'objet d'un droit d'auteur (articles de revue, tests publiés, etc.) ne sont pas microfilmés.

La reproduction, même partielle, de cette microforme est soumise à la Loi canadienne sur le droit d'auteur, SRC 1970, c. C-30.

Stream Function-Vorticity-Pressure Functional
Solution of the Steady Euler Equations

Zhigang Fang

A Thesis

in

The Department

of

Mechanical Engineering

Presented in Partial Fulfillment of the Requirements
for the Degree of Doctor of Philosophy at
Concordia University
Montréal, Québec, Canada

June 1988

© Zhigang Fang, 1988

Permission has been granted to the National Library of Canada to microfilm this thesis and to lend or sell copies of the film.

The author (copyright owner) has reserved other publication rights, and neither the thesis nor extensive extracts from it may be printed or otherwise reproduced without his/her written permission.

L'autorisation a été accordée à la Bibliothèque nationale du Canada de microfilmer cette thèse et de prêter ou de vendre des exemplaires du film.

L'auteur (titulaire du droit d'auteur) se réserve les autres droits de publication; ni la thèse ni de longs extraits de celle-ci ne doivent être imprimés ou autrement reproduits sans son autorisation écrite.

ISBN 0-315-44887-3

ABSTRACT.

ABSTRACT

Stream Function-Vorticity-Pressure Functional
Solution of the Steady Euler Equations

Zhigang Fang, Ph.D.
Concordia University, 1988

In this thesis, a new variable is proposed to couple the stream function-vorticity formulation of the steady Euler equations. The development of the variable designated the pressure functional and its employment in a stream function-vorticity formulation of the steady Euler equations are shown. The partial differential equation relating the new variable to other variables of the flow field is derived from the steady Euler momentum equation. Boundary conditions for this variable are very straightforward to implement when the finite element weighted residual method is employed. With this formulation, the difficulty encountered when stream function formulation is applied to transonic internal flow calculations is overcome easily. This formulation is applied not only to internal but also to external flows. The solution procedure for this variable is very similar to that for velocity potential. However, in contrast to the velocity potential, rotational effects are taken into account.

To achieve this purpose, the stream function and vorticity method for solving compressible inviscid flow problems is studied in this thesis. The resulting vorticity transport equation is proved to be valid for inviscid flows of an ideal gas. For two dimensional flows, the vorticity transport equation reduces to a vorticity conservation form. It states that the ratio of vorticity to pressure is a constant along a stream line.

In this study, a finite element solution procedure for the first order vorticity transport equation is also discussed, because the Galerkin weighted residual approach for first order partial differential equations will lead to a singular matrix system as the central finite difference does. Two procedures to handle the vorticity transport equation are discussed. First, the vorticity transport equation is solved simultaneously with the stream function equation. Second, the second order vorticity transport equation is solved. In the latter case, an auxiliary boundary condition must be satisfied as the compensation for the increase of partial differential equation order.

A particular result is that for transonic flow, a sharp shock can be found with the new variable formulation.

ACKNOWLEDGEMENTS

ACKNOWLEDGEMENTS

The author wishes to express his appreciation to Dr. A. J. Saber for his guidance and support in the course of this investigation.

Assistance of Huazhong University of Science and Technology which was provided in the form of one year scholarship funding is greatly appreciated. This research project was partially funded by the NRC under Grant No. A5700.

The author also wishes to thank Computer Center of Concordia University for the computer service.

Finally, the author wishes to express his appreciation to the Faculty of Engineering and Computer Science and his colleagues for their courses, valuable discussions and encouragement.

CONTENTS

CONTENTS

Abstract.....	iii
Acknowledgements.....	v
Contents.....	vi
List of tables and figures.....	viii
Nomenclature.....	xi

CHAPTER 1.

INTRODUCTION

1.1 Purpose of this research.....	3
1.2 A brief history of the finite element method.....	5
1.3 Numerical solution of compressible inviscid..... flow problems.....	7
1.4 Stream function and vorticity method.....	11
1.5 Outline of this thesis.....	14

CHAPTER 2.

GOVERNING EQUATIONS

2.1 The basic equations.....	19
2.2 Vorticity transport equation.....	22
2.3 Stream function formulation.....	26
2.4 Pressure functional method.....	28

CHAPTER 3.

FINITE ELEMENT SOLUTION ALGORITHM

3.1 Solutions using the finite element method.....	32
3.2 Finite element formulation of SF-V-Q equations..	34

3.3 Assembly of the matrix.....	38
3.4 Solution procedure.....	43
3.5 Boundary conditions.....	45

CHAPTER 4.

SOLUTION EXAMPLES

4.1 An introductory discussion.....	47
4.2 Quasi-one dimensional nozzle flow.....	50
4.3 Two dimensional nozzle flow.....	54
4.4 External flows.....	60

CHAPTER 5.

CONCLUDING REMARKS

5.1 Pressure functional method.....	65
5.2 Stream function-vorticity formulation.....	67
5.3 Conservation of the vorticity.....	68
5.4 Solution technique.....	70
5.5 Numerical results.....	72
5.6 Final comments.....	73
References.....	74
Tables and figures.....	87

LIST OF TABLES AND FIGURES

LIST OF TABLES AND FIGURES

- Fig. 1. Stream lines of irrotational flow
- Fig. 2. Stream lines of rotational flow
- Fig. 3. Mach numbers along the nozzle
- Fig. 4. Pressure distribution along the nozzle
- Fig. 5. Mach number along the nozzle for transonic flow
- Fig. 6. Pressure distribution along the nozzle
for transonic flow
- Fig. 7. Finite element mesh for a two dimensional
nozzle flow
- Fig. 8. Inlet velocity ratio profiles
- Fig. 9. Pressure profiles at the throat for different
inlet Mach numbers
- Fig. 10. Nozzle stream lines
- Fig. 11. Vorticity along the nozzle boundary
- Fig. 12. Mach number along the nozzle, flow type
- Fig. 13. Mach number along the nozzle, flow type
- Fig. 14. Pressure distribution along the nozzle
- Fig. 15. Pressure distribution along the nozzle
- Fig. 16. Lines of equal vorticity
- Fig. 17. Lines of equal vorticity
- Fig. 18. Coarse grid for NACA-0012 airfoil
- Fig. 19. Refined grid for NACA-0012 airfoil
- Fig. 20. Pressure coefficient on NACA-0012 airfoil,
 $M_\infty=0.5$

- Fig. 21. Pressure coefficient on NACA-0012 airfoil,
 $M_\infty=0.703$
- Fig. 22. Pressure coefficient on NACA-0012 airfoil,
 $M_\infty=0.803$
- Fig. 23. Pressure coefficient on NACA-0012 airfoil,
 $M_\infty=0.829$
- Fig. 24. Pressure coefficient on NACA-0012 airfoil,
 $\alpha=2.06, M_\infty=0.502$
- Fig. 25. Pressure coefficient on NACA-0012 airfoil,
 $\alpha=1.95, M_\infty=0.753$
- Fig. 26. Pressure coefficient on NACA-0012 airfoil,
 $\alpha=2.98, M_\infty=0.754$
- Fig. 27. Convergence history for NACA-0012 airfoil,
 $M_\infty=0.703$
- Fig. 28. Convergence history for NACA-0012 airfoil,
 $M_\infty=0.803$
- Fig. 29. C_p comparison for refined grid,
 $M_\infty=0.703$
- Fig. 30. C_p comparison for refined grid,
 $M_\infty=0.803$

NOMENCLATURE



NOMENCLATURE

ρ	Density of the fluid
ρ_0	Stagnation density of the fluid
\bar{V}	Velocity vector
$ \bar{V} $	Magnitude of the velocity
u	Velocity component in x direction
v	Velocity component in y direction
w	Velocity component in z direction
γ	Ratio of the specific heat
h	Enthalpy of the fluid
h_0	Stagnation enthalpy of the fluid
$\bar{\omega}$	Vorticity vector
ω	Vorticity in x-y plane
t	Time
Γ	Circulation
∇	Vector differential operator
ψ	Stream function in two dimensional field
ψ_1	Stream function in three dimensional field
ψ_2	Stream function in three dimensional field
x, y, z	Cartesian coordinates
Q	Pressure potential
W	Weighting function
N_i	Shape function
n	Normal direction of stream lines
s	Tangential direction of stream lines

$K_{i,j}^e$	Local stiffness matrices
U_∞	Free stream velocity
ρ_∞	Free stream density
α	Airfoil attack angle
A	Global matrix
\bar{F}	Right hand side vector
\bar{G}	Variable vector
a_0	Stagnation sound velocity

CHAPTER 1

INTRODUCTION

CHAPTER 1.

INTRODUCTION

The Navier-Stokes equations describe the flows commonly encountered in engineering problems. However, it is impractical in many applications, or impossible in some cases today, to solve the equations completely. Nevertheless, if viscosity can be neglected, the Navier-Stokes equations reduce to the Euler equations. Numerical solutions of the Euler equations are particularly useful in some engineering problems where information on pressure alone is desired.

One method for solving the Euler equations is the stream function formulation. However, when stream function formulations are used for internal transonic flows the nozzle back pressure cannot be matched. As a result, shocks which might occur in reality cannot be trapped numerically.

In this thesis, a new variable which can be called the pressure functional is proposed to overcome the difficulty encountered when the stream function formulation is used to

solve internal transonic flows. This new formulation can also be used for external flows.

The presentation includes a study of the stream function-vorticity formulation of the steady Euler equations, and the vorticity nature of compressible inviscid flows. The Euler equations are solved for two dimensional subsonic and transonic internal and external flows using the finite element method. Based on the results of the solution, statements about compressible inviscid flows are made and directions for future developments are suggested.

1.1 Purpose of this research

Internal nozzle flows occur in industrial applications including supersonic wind tunnels and jet engine inlet diffusers.¹ These applications require both experimental trials and calculations to create designs. The calculations involve approximations to the complete Navier-Stokes equations. Nevertheless, it is both time consuming and costly to obtain the solutions of the Navier-Stokes equations. In particular, in one approximation, the velocity potential has been employed. However, the results of that application of the velocity potential are limited because of the irrotational flow assumption.

Stream function formulations are excellent substitutes for the velocity potential formulation. This is because the stream function formulation is straightforward to modify to account for rotational effects. Nevertheless, this method requires knowledge of the vorticity, although the vorticity is not known without a properly posed vorticity equation.

Furthermore, as mentioned above, when stream function formulations are used to solve internal transonic nozzle flows, it is extremely difficult to trap shocks because the formulation cannot match the nozzle back pressure. This difficulty is resolved in this work by using a variable called the pressure functional. This variable is used to

couple the stream function-vorticity formulation for pressure updating. The nozzle back pressure can then be used to determine the boundary conditions. Using the pressure functional easily bypasses the difficulty encountered in stream function solutions of transonic internal nozzle flows.

The numerical approach employed uses the finite element method.

1.2 A brief history of the finite element method

The finite element method is an efficient numerical procedure for solution of the differential equations of engineering mechanics. This numerical solution algorithm has been used extensively in analysis and design procedures in engineering and industry.

This solution procedure was originally developed by structural engineers in the 1950's to analyze large structural systems for aircraft. Turner, et al. presented the first paper on this subject.² Other authors involved in the early research were Clough³ and Argyris.⁴

Applications of the finite element method to a wide class of nonlinear mechanics problems were contributed by Oden.⁶ Other important research was done by Babuska and Aziz,⁷ Ciarlet and Raviart,⁸ Aubin,⁹ Strang and Fix,¹⁰ and Lions and Magenes.¹¹

In the last fifteen years, finite element solutions of fluid flow problems have been studied extensively. Application of the finite element method to fluid flow problems was first reported by Zienkiewicz and Cheung.⁵ Other pioneering research on applications to fluid mechanics problems were undertaken by Oden,⁶ Cheng,¹² Chan and Larock,¹³ Baker,¹⁴ Olson,¹⁵ Doctors,²⁵ Norrie and Vries.²⁶

In 1978, Chung published the first book on this subject,¹⁶ and in 1983, Baker published another book in this field.¹⁷

We apply the method to transonic compressible flow problems.

1.3 Numerical solution of compressible inviscid flow problems

Numerical modeling of compressible inviscid flow problems is a very important branch of applied aerodynamics and fluid dynamics. Using these methods, as indicated by Salas,¹⁸ a large number of external aerodynamic problems can be accurately described by a simple model consisting of an outer inviscid flow plus a boundary-layer thickness correction for the vehicle shape.

At the start of last decade, numerical solutions were mainly carried out by the finite difference method. The research work included a mixed finite difference scheme for solving the transonic small-perturbation equation for the velocity potential by Murman and Cole.¹⁹ This was considered a breakthrough in the field of computational transonics.²⁰

Later, the transonic full potential equation was studied by many researchers using both finite difference and finite element methods. The methods included development of the so called artificial viscosity method for transonic flows. It is still used in many full potential codes today. Basically, the artificial viscosity method is derived from Jameson's method for the conservative transonic potential calculation.²¹ This method was further studied by Hafez et al.,²² Holst and Ballhaus,²³ and Purvis and Burkhalter.²⁴

Early applications of finite element solutions of transonic full potential equation were studied by Deconinck and Hirsch,²⁷ Bristeau et al.,²⁸ Eberle,²⁹ and Habashi.³⁰ Finite element solutions of the stream function equation have also been studied by Habashi and Hafez,³¹ and Hafez and Lovell.³²

Applications of these methods to turbomachinery were presented by Deconinck and Hirsch,³³ Habashi and Hafez,³¹ Steger et al.,³⁴ Keck and Haas,³⁵ Habashi and Youngson,³⁶ and Cedar and Stow.³⁷ However, because the full potential equation is based on the assumption that the flow is irrotational, it does not account for the rotational effects. Furthermore, it has been found that the solution of the full potential equation is not unique. For certain values of angle of attack and Mach number, the basic transonic potential equation admits two or three solutions for the lift.^{38,43} Therefore, application of the full potential equation is limited.

Because the full-potential equation does not account for rotational effects, a modified potential method was studied by Habashi, Hafez and Kotiuga.^{53,54} Using the modified potential, the pressure is calculated by solving the Euler momentum equations rather than the density-velocity relation. It is reported in their papers that for transonic flows over an airfoil with an attack angle, the modified

potential gives a unique solution. However, the modified potential method predicts no sharp shock waves when transonic flow problems are solved. Shock waves are smeared over a number of elements.

Both modified stream function and other stream function formulations have been studied.^{32,55,56,57,58} These studies show that stream function formulations are excellent substitutes for the full potential equation, since agreement between the full potential and the stream function equation is good. However, in contrast to the full potential, the stream function formulation can easily be modified to account for rotational effects.

Most of the modified stream function formulations are based on Crocco's relation. This method requires knowledge of the vorticity. However, vorticity is not known without a properly posed vorticity equation.

In the past, solutions of the Euler equations were studied mainly by finite difference method and finite volume method.^{39,40,41,42,44,45,46} As pointed out by Steger and Warming⁵¹ and Johnson⁵², attempts to deal directly with the steady first order Euler equations have met with immediate difficulties. Thus, some alternative approaches were studied, such as semi-direct solution procedures⁴⁶ and high order embedded method.^{44,45}

The steady Euler equations are also difficult to solve with the finite element method. This is mainly because a set of first order partial differential equations are involved. The Galerkin weighted residual approach for these first order partial differential equations will lead to a singular matrix system as the central finite difference does. Finite Element least square method for solving the steady and the unsteady Euler equations was studied.^{47,48} Other forms of the Euler equations are also studied, such as the use of Clebsch-type variables.^{49,50} The above studies have led toward alternative implementations of the Euler equations.

1.4 Stream function and vorticity method

The stream function and vorticity method for solving the Navier-Stokes equations has been studied by many researchers.⁵⁹⁻⁶⁹ Unfortunately, most of these studies are for incompressible flow problems. In 1972, Cheng⁵⁹ applied the stream function and vorticity method to incompressible viscous flows. Following Cheng, the stream function-vorticity method was studied and applied to the incompressible Navier-Stokes flow problems. These studies were limited to low Reynolds number flows. Now, it is well known that this limitation is caused by the solution procedure.^{63,65,67} However, at that time, researchers did not recognize this. Olson and Tuann⁶² claimed that in the stream function-vorticity method, the discretized equations for the stream function and the vorticity cannot be solved simultaneously because vorticity boundary conditions are not known *a priori*. This opinion was in accordance with the paper by Taylor and Hood.⁶¹ In that paper, they proposed an iterative technique for satisfying the vorticity boundary conditions. These solution procedures for the stream function and vorticity equations reduced the stability of iterations. Thus, the stream function and vorticity method was limited to very low Reynolds number flow problems,

Later studies show that if the solution procedure is changed, it is possible to apply the stream

function-vorticity method to high Reynolds number flows.⁶³ It is also found out that the stream function-vorticity equations allow for solving their discretized form simultaneously.^{65,67} When solving the stream function equation and the vorticity transport equation simultaneously, there is no convergence problem. The Reynolds number can be higher than the laminar flow limit. Vorticity boundary conditions along body boundaries are determined by stream function solutions in the nearby region of the solid wall. We observed that the stream function-vorticity method for incompressible viscous flow problems has been studied only for two dimensional flow problems.

Peeters et al.,⁶⁷ proposed a new procedure for implementation of the boundary conditions of the stream function-vorticity formulation. In that paper, the no-slip solid wall boundary condition is applied by taking advantage of the simple implementation of natural boundary conditions in the finite element formulation. The iterative evaluation of wall vorticity is not needed. The extension of this method to compressible two dimensional flows has been studied by Habashi, et al.⁶⁹

Although the stream function-vorticity method has been applied to both incompressible and compressible flows, the details of formulation of this method for compressible

inviscid flow problems remain unknown. In this work, it is found that the stream function-vorticity method is a very efficient and useful approach for compressible inviscid flows. The vorticity transport equation for compressible inviscid flows provides an important clue for understanding the vorticity nature of compressible inviscid flows.

1.5 Outline of this thesis

The steady Euler equations with primitive variables are very difficult to solve with the finite element method. This is because the Galerkin weighted residual finite element approach, like the central finite difference method, will generate a singular matrix system. For this reason, other forms of the Euler equations are studied. In this work, the stream function and vorticity formulation is applied for solving the steady Euler equations. This approach involves invoking the vorticity transport equation for compressible inviscid flows. The vorticity transport equation for compressible inviscid flows is derived from the Euler equations. For two dimensional compressible flows, the equation states that the ratio of vorticity to pressure remains constant along a stream line.

It was indicated above that most of the inviscid transonic flow solutions introduce the vorticity explicitly, but only after the shock wave. However, according to the vorticity transport equation studied in this work, the vorticity is conserved for two dimensional flows. Thus, vorticity introduced across the shock wave must be carried infinitely, because there is no vorticity dissipation in the inviscid flows governed by the Euler equations.

The vorticity transport equation studied in this work is a first order partial differential equation. To include such a first order partial differential equation in a numerical procedure requires an efficient solution algorithm. Therefore, in this study, the vorticity transport equation is handled by two different solution procedures. In the first procedure, the stream function equation and the vorticity transport equation are solved simultaneously. The Galerkin weighted residual approach can be used for both the stream function equation and the vorticity transport equation. In this case, the matrix is not ill-conditioned because the vorticity term involved in the stream function equation is dependent on the vorticity transport equation. The second approach is to solve the second order form of the vorticity transport equation. In this case, the stream function equation and the vorticity transport equation can be solved separately. However, an auxiliary boundary condition must be satisfied as the compensation for the increase of the partial differential equation order. In this work, it is shown that the auxiliary boundary condition is straightforward to handle with the finite element method because the boundary integral in the finite element formulation of the second order vorticity transport equation vanishes.

Next, a new formulation for internal transonic flows is proposed based on a new variable definition. This new variable can be called 'pressure functional'. Physically, the pressure functional represents the work done by the fluid along a stream line. The purpose of this formulation is to couple the stream function-vorticity formulation for internal transonic flow calculations.

The presentation proceeds to the partial differential equation relating the pressure functional and variables of the flow field. It too is derived from the steady Euler equations. Boundary conditions for the pressure functional equation are very easy to implement when finite element weighted residual method is employed since boundary conditions along stream line boundaries or body boundaries are Neumann boundary conditions. In the finite element formulation, Neumann boundary conditions are straightforward to implement since boundary integrals appearing in finite element equations are null. It is also interesting to observe that upstream inlet and downstream outlet boundary conditions for this variable are very similar to those of the velocity potential for internal flows. Free stream boundary conditions for external flows also take similar forms. The solution procedure is very similar to the one used for the velocity potential for both subsonic and transonic internal flows.⁷⁰ For transonic flows, pressure

functional values must be specified at both inlet and outlet. The increase of the pressure functional values between inlet and outlet is uniquely determined by the nozzle exit back pressure.

This thesis includes two calculations. The first is the transonic internal nozzle flow. The second is the transonic flow over the NACA-0012 airfoil.

CHAPTER 2

GOVERNING EQUATIONS

CHAPTER 2.

GOVERNING EQUATIONS

In this chapter, we discuss the Euler equations, namely the basic equations for inviscid flows and continue to discuss the stream function-vorticity-pressure functional formulation of the steady Euler equations.

2.1 The basic equations

The conservation laws for compressible inviscid fluid flows are described by the Euler equations. These equations demonstrate how the mass, momentum, and energy are conserved in the flow field.

The continuity equation is

$$\frac{D\rho}{Dt} + \rho \nabla \cdot \bar{V} = 0 \quad (2-1)$$

where ρ is density, \bar{V} is the velocity vector, and t is time.

The operator

$$\frac{D}{Dt} = \frac{\partial}{\partial t} + \bar{V} \cdot \nabla \quad (2-2)$$

denotes that the derivative is taken following the fluid particles.

The momentum equation can be written as

$$\frac{D\bar{V}}{Dt} + \frac{1}{\rho} \nabla P = 0 \quad (2-3)$$

where P is the pressure and all external body forces are neglected.

If there is no heat conduction in inviscid flows, the energy equation can be written as

$$\frac{Dh}{Dt} = \frac{1}{\rho} \frac{DP}{Dt} \quad (2-4)$$

where h is the enthalpy. If the inviscid fluid is also a perfect gas, the energy equation can be written as

$$\frac{DP}{\rho Dt} = \gamma P \frac{D\rho}{Dt}, \quad (2-5)$$

where $\gamma = c_p/c_v$. This equation can also be written as

$$P/\rho^\gamma = \text{constant (along a stream line)}. \quad (2-6)$$

Equation (2-6) is valid for compressible inviscid non-heat conducting flows of the perfect gas. If the upstream stagnation condition is uniform, equation (2-6) is valid through the entire field.

By taking the scalar product of the velocity vector and the momentum equation, we can obtain

$$\bar{V} \cdot \left(\frac{D\bar{V}}{Dt} + \nabla P/\rho \right) = 0. \quad (2-7)$$

Therefore, we have

$$D(\bar{V}^2/2)/Dt + \frac{1}{\rho} \bar{V} \cdot \nabla P = 0. \quad (2-8)$$

For steady flows, the energy equation and the momentum equation combine to yield

$$\bar{V} \cdot \nabla h + \bar{V} \cdot \nabla (v^2/2) = 0. \quad (2-9)$$

This equation states that the total enthalpy is a constant along a stream line in steady flows. If the fluid is a perfect gas, the energy equation becomes

$$\gamma P / ((\gamma - 1)\rho) + \frac{1}{2}v^2 = \text{constant} \quad (2-10)$$

along a stream line. This form of the steady energy equation is frequently used for solving compressible inviscid flow problems. Other forms of the Euler equations are discussed by by Salas¹⁸, and Moretti⁷³, for example.

2.2 Vorticity transport equation

The vorticity transport equation, which represents conservation of vorticity, can be derived from momentum equations. The definition of the vorticity vector in any orthogonal coordinate system is

$$\bar{\Omega} = \nabla \times \bar{V} \quad (2-11)$$

where $\bar{\Omega}$ is the vorticity vector, \bar{V} is the velocity of the flow, and ∇ is the gradient operator.

Since the momentum equation for compressible inviscid flows can be written as

$$\frac{\partial \bar{V}}{\partial t} + (\bar{V} \cdot \nabla) \bar{V} = - \frac{\nabla P}{\rho}, \quad (2-12)$$

the convective term in the momentum equation can be expressed in the following way

$$\nabla(\bar{V} \cdot \bar{V}) = 2\bar{V} \cdot \nabla \bar{V} + 2\bar{V} \times (\nabla \times \bar{V}) \quad (2-13)$$

or

$$(\bar{V} \cdot \nabla) \bar{V} = \frac{1}{2} \nabla V^2 - \bar{V} \times \bar{\Omega}. \quad (2-14)$$

Substituting equation (2-14) into equation (2-12), we can obtain

$$\frac{\partial \bar{V}}{\partial t} = \bar{V} \times \bar{\Omega} - \left(\frac{1}{2} \nabla V^2 + \frac{\nabla P}{\rho} \right). \quad (2-15)$$

Taking the curl of each term in equation (2-15), we can obtain the following equation

$$\frac{\partial \bar{\Omega}}{\partial t} = \nabla \times (\bar{V} \times \bar{\Omega}) - \left(\nabla \frac{1}{\rho} \right) \times \nabla P. \quad (2-16)$$

In equation (2-16)

$$\nabla \times (\bar{V} \times \bar{\Omega}) = (\bar{\Omega} \cdot \nabla) \bar{V} - (\bar{V} \cdot \nabla) \bar{\Omega} - \bar{\Omega} (\nabla \cdot \bar{V}) \quad (2-17)$$

and by perfect gas equation

$$-\nabla (1/\rho) \times \nabla P = -\nabla T \times \nabla P / (\rho T) \quad (2-18)$$

From thermodynamic relation

$$\nabla P / \rho = \nabla h - T \nabla S \quad (2-19)$$

equation (2-18) becomes

$$-\nabla(1/\rho) \times \nabla P = \nabla T \times \nabla S \quad (2-20)$$

Thus, equation (2-16) can be written as

$$\begin{aligned} \frac{D(\bar{\Omega}/\rho)}{Dt} &= \left(\frac{\bar{\Omega}}{\rho} \cdot \nabla\right) \bar{V} \\ &+ \nabla T \times \nabla S / \rho \end{aligned} \quad (2-21)$$

For steady isoenergetic flow, Crocco equation is

$$\bar{\Omega} \times \bar{V} = T \nabla S \quad (2-22)$$

Thus,

$$\begin{aligned} \nabla T \times \nabla S &= \nabla T \times (\bar{\Omega} \times \bar{V}) / T \\ &= (\bar{\Omega}(\bar{V} \cdot \nabla T) - \bar{V}(\bar{\Omega} \cdot \nabla T)) / T \end{aligned} \quad (2-23)$$

Using equation (2-23), equation (2-21) is written as

$$\begin{aligned} (1/T) \frac{\partial(\bar{\Omega}/\rho)}{\partial t} + \bar{V} \cdot \nabla \frac{\bar{\Omega}}{\rho T} \\ = (1/\rho) \bar{\Omega} \cdot \nabla (\bar{V}/T) \end{aligned} \quad (2-24)$$

For steady two dimensional flow, equation (2-24) reduces to

$$\bar{V} \cdot \nabla \frac{\omega}{\rho T} = 0 \quad (2-25)$$

where $\omega = v_x - u_y$.

Thus, the ratio of vorticity to pressure is a constant along a stream line⁷⁴

$$\bar{V} \cdot \nabla \frac{\omega}{P} = 0 \quad (2-26)$$

Equation (2-26) not only states that if a flow begins irrotationally, it will remain irrotational through the entire two dimensional flow field, but also describes the relation of vorticity to pressure.

For steady flows, the vorticity transport equation can also be written in second order form as

$$\rho \bar{V} \cdot \nabla \left\{ \rho \bar{V} \cdot \nabla \left(\frac{\omega}{P} \right) \right\} = 0. \quad (2-27)$$

2.3 Stream function formulation

For three dimensional flows, two stream functions are needed because one scalar value function in a three dimensional flow field cannot determine stream line patterns. These two scalar functions are two stream surfaces in a three dimensional flow field. Their intersection contour represents a stream line.

If these two functions are expressed by Ψ_1 and Ψ_2 , the compressible velocity field is given by

$$\rho \bar{V} = \nabla \Psi_1 \times \nabla \Psi_2. \quad (2-28)$$

Since vorticity is the curl of the velocity,

$$\bar{\Omega} = \nabla \times ((\nabla \Psi_1 \times \nabla \Psi_2) / \rho). \quad (2-29)$$

If the flow field is reduced to two dimensions, we have

$$\Psi_2 = z \quad (2-30)$$

and

$$\Psi_1 = f(x, y). \quad (2-31)$$

The above equations then reduce to

$$\rho u = \frac{\partial \psi}{\partial y} \quad (2-32)$$

and

$$\rho v = - \frac{\partial \psi}{\partial x}. \quad (2-33)$$

This is the classical two dimensional definition of the velocity field. The stream function equation becomes

$$\nabla \cdot \left(\frac{1}{\rho} \nabla \psi \right) + \omega = 0. \quad (2-34)$$

To close the set of partial differential equations for a complete formulation of compressible flow problems, equations for pressure and density are also required.

2.4 Pressure functional method

A pressure relation can be derived from the momentum equation. By taking the divergence of the momentum equation, we get

$$\nabla^2 p = - \nabla \cdot (\rho (\bar{V} \cdot \nabla) \bar{V}). \quad (2-35)$$

As indicated by Hafez, et al.,⁵⁴ if this formulation is employed for transonic flow problems, no sharp shock can be found:⁵⁴ The shock is smeared over a number of elements.

In this work, we introduce a new formulation in order to trap sharp shocks. The new variable introduced in this work can be called 'pressure functional'. The governing partial differential equation for the pressure functional can be derived from the momentum equation. With this new variable, finite element discretization can be done easily.

The pressure functional Q is defined by

$$P = \frac{\bar{V}}{|\bar{V}|} \cdot \nabla Q \quad (2-36)$$

where P is the local pressure in the flow field. By taking the scalar product of the velocity vector with the

divergence of equation (2-36); we obtain

$$\rho \bar{V} \cdot \nabla \left(\frac{\bar{V}}{|\bar{V}|} \cdot \nabla Q \right) = \rho \bar{V} \cdot \nabla P. \quad (2-37)$$

Using the momentum equation for steady flows written as

$$\rho (\bar{V} \cdot \nabla) \bar{V} = - \nabla P \quad (2-38)$$

in equation (2-37), we have

$$\rho \bar{V} \cdot \nabla \left(\frac{\bar{V}}{|\bar{V}|} \cdot \nabla Q \right) = - \rho^2 \bar{V} \cdot (\bar{V} \cdot \nabla) \bar{V}. \quad (2-39)$$

Equation (2-39) provides a required necessary relation between the pressure functional and the velocity of the flow field.

For subsonic flows, both the pressure equation and the pressure functional equation can be solved and both formulations give the same solution. For transonic flows, pressure is calculated by solving the pressure functional equation above. Our results indicate that employing the finite element-weighted residual discretization method, the pressure functional demonstrates a similar behaviour to the velocity potential, for internal transonic flow problems. So, the difficulty encountered in the solution procedure of

the internal transonic stream function formulation disappears.

After the pressure is obtained, the density is calculated using the energy equation.

CHAPTER 3

FINITE ELEMENT SOLUTION ALGORITHM

CHAPTER 3.

FINITE ELEMENT SOLUTION ALGORITHM

Most of partial differential equations that describe fluid flows are nonlinear and may have complex or unknown initial and boundary conditions. This makes fully analytical solution of real engineering problems impractical at this time. Nevertheless, today's technological equipment still demands solutions of these partial differential equations. These solutions can be determined by numerical procedures. One of the procedures is the finite element method.

The finite element method is a solution method based on a numerical discretization of a mathematical statement such as a variational principle. When variational principles are not available, a weighted residual formulation or a least square method is used as an approximation.

In this thesis, a finite element solution procedure using a weighted residual formulation is applied to solve those equations for two dimensional, subsonic and transonic flows both over airfoils and in channels.

3.1 Solutions using the finite element method

The finite element method was originally developed to solve differential equations numerically by employing variational principles. However, for a large class of partial differential equations encountered in engineering problems, there is no variational principle. An alternative developed to preclude this difficulty is the Galerkin weighted residual formulation.¹⁷ In this work, the Galerkin weighted residual method is used for the finite element formulation.

With the Galerkin weighted residual method, a partial differential equation is written so that zero occurs on one side of the equal sign; if an exact solution could be substituted into the equation, the result would be zero. However, the exact solution is not known for most partial differential equations in engineering problems. Accordingly, if an approximation to the exact solution is substituted into the differential equation, an erroneous value results. In the procedure, this error is multiplied by a weighting function and the product is integrated over the solution region and set equal to zero.

The next step is to divide the solution region into appropriately shaped elements. This process is called grid generation. Then, within each element, the physical

variable is approximated by a simple function. Thus, the variable within an element may be approximated by a linear combination of element values at the nodes variables. The coefficients of the nodal values are called shape functions. In each element, a local stiffness matrix is formed in accordance with the nodal values of the physical variable.

The entire field is then characterized by a global matrix constituted from local matrices. This forms a set of algebraic equations for the nodal values of the physical variable. The solution of the algebraic equations provides the solution for the field.

For nonlinear partial differential equations, an iterative procedure is required because the global matrix is dependent on the physical variable.

3.2 Finite element formulation of SF-V-Q equations

The vorticity transport equation is a first order partial differential equation. In the previous chapter, it is indicated that the Galerkin weighted residual finite element method will give the same discretized simultaneous equations as does the central finite difference for first order partial differential equations. Thus, the solution procedure is unstable or oscillates in the stream line direction. Two approaches can be used to overcome this difficulty. In the first approach, the stream function equation and the vorticity transport equation are solved simultaneously with the Galerkin weighted residual method. However, since the vorticity transport equation is coupled with the stream function equation solutions of the discretized simultaneous equations of the vorticity transport equation are not independent. The second approach solves the second order form of the vorticity transport equation. Here, however, stream function equation and vorticity equation can be solved independently.

The Galerkin weighted residual formulations for these equations are

$$\int [W(\nabla \cdot (\frac{1}{\rho} \nabla \psi) + \omega)] dx dy = 0 \quad (3-1)$$

for stream function equation,

$$\iint W(\rho \bar{V} \cdot \nabla \frac{\omega}{\rho}) dx dy = 0 \quad (3-2)$$

for vorticity transport equation, equation (2-19),

$$\iint W \rho \bar{V} \cdot \nabla (\rho \bar{V} \cdot \nabla \frac{\omega}{\rho}) dx dy = 0 \quad (3-3)$$

for the second order vorticity transport equation, equation (2-20),

$$\iint W V^2 P dx dy = \iint W f dx dy \quad (3-4)$$

for pressure equation, equation (2-35) and

$$\begin{aligned} \iint W \rho \bar{V} \cdot \nabla \left(\frac{\bar{V}}{|\bar{V}|} \cdot \nabla Q \right) dx dy \\ = \iint W f_1 dx dy \end{aligned} \quad (3-5)$$

for pressure functional equation, equation (2-39). In the above relations, f is the right hand side of the pressure equation, f_1 is the right hand side of the pressure functional equation, and W is the weighting function.

Carrying out the Green transformation, we can obtain the following equations

$$\iint \left(\frac{1}{\rho} \nabla \psi \cdot \nabla W - W \omega \right) dx dy$$

$$= \int_{\Gamma} \frac{W \partial \psi}{\rho \partial n} ds \quad (3-6)$$

for stream function equation,

$$\iint W \bar{V} \cdot \nabla_{\bar{p}} \frac{\omega}{\rho} dx dy = 0 \quad (3-7)$$

for vorticity transport equation,

$$\begin{aligned} \iint (\rho \bar{V} \cdot \nabla_{\bar{p}} \frac{\omega}{\rho}) (\rho \bar{V} \cdot \nabla W) dx dy \\ = \int_{\Gamma} W \rho \bar{V} \cdot \nabla_{\bar{p}} \frac{\omega}{\rho} V_n ds \end{aligned} \quad (3-8)$$

for the second order vorticity transport equation,

$$\begin{aligned} \iint (\nabla P) \cdot (\nabla W) dx dy = \iint (\nabla W) \cdot (\rho \bar{V} \cdot \nabla \bar{V}) dx dy \\ + \int_{\Gamma} W (\rho \bar{V} \cdot \nabla \bar{V} + \nabla P)_n ds \end{aligned} \quad (3-9)$$

for pressure equation, and

$$\begin{aligned} \iint \left(\frac{\bar{V}}{|\bar{V}|} \cdot \nabla Q \right) (\rho \bar{V} \cdot \nabla W) dx dy \\ = - \iint (\nabla \rho) \cdot \nabla \bar{V} \cdot \nabla W dx dy + \int_{\Gamma} W \rho (\rho V^2 + p) V_n ds \\ - \iint W \rho \bar{V} (\bar{V} \cdot \nabla) \rho \bar{V} dx dy \end{aligned} \quad (3-10)$$

for pressure functional equation, where $\int_{\Gamma} ds$ represents an integral along the positive direction of the field boundary, and n is the normal direction of the boundary.

If the second order vorticity transport equation is solved, the partial differential equation switches from first order to second order. This implies an auxiliary boundary condition,

$$\bar{V} \cdot \nabla \frac{\xi}{p} = 0. \quad (3-11)$$

Thus, the boundary integral of the right hand side of equation (3-8) disappears.

3.3 Assembly of the matrix

The simultaneous equations are constituted from the local stiffness matrices. Within an element, the weighting function is chosen to be the element shape function...

In this study, isoparametric bilinear elements with four nodes are used with the following approximations:

$$\psi(x,y) = N_i(x,y)\psi_i^e \quad (i=1,2,3,4) \quad (3-12)$$

$$\frac{\omega}{p}(x,y) = N_i(x,y)(\omega/p)_i^e \quad (3-13)$$

$$P(x,y) = N_i(x,y)P_i^e \quad (3-14)$$

or for pressure functional

$$Q(x,y) = N_i(x,y)Q_i^e \quad (3-15)$$

where ψ_i^e , $(\omega/p)_i^e$, P_i^e and Q_i^e are nodal values of the element e .

The discretized simultaneous equations are assembled by the following local stiffness matrices. For coupled stream function and vorticity, the local stiffness matrix is

$$K_{i,j}^e(\psi,\psi) + K_{i,j}^e(\psi,\omega/p) = f^e \Gamma(\psi) \quad (3-16)$$

$$K_{i,j}^e(\frac{\omega}{p}, \frac{\omega}{p}) = 0 \quad (3-17)$$

where

$$K_{i,j}^e(\psi, \psi) = \iint \frac{1}{\rho} (\nabla N_i) \cdot (\nabla N_j) dx dy \quad (3-18)$$

$$K_{i,j}^e(\psi, \frac{\omega}{p}) = -\iint N_i N_j dx dy \quad (3-19)$$

$$\begin{aligned} K_{i,j}^e(\frac{\omega}{p}, \frac{\omega}{p}) \\ = \iint N_i (\rho V \cdot \nabla N_j) dx dy \end{aligned} \quad (3-20)$$

and

$$f_{\Gamma}^e(\psi) = \int_{\Gamma} N_i / \rho \cdot \frac{\partial \psi}{\partial n} ds \quad (3-21)$$

In these equations, $f_{\Gamma}^e(\psi)$ only appears on boundary elements.

For the second order vorticity transport equation, the vorticity term in the stream function equation appears on the right hand side and is updated in the subsequent iterations. The boundary integral of the vorticity formulation disappears. Thus, the auxiliary boundary condition is satisfied as compensation for the increase of the vorticity transport equation order. The local stiffness

matrix in this case is

$$K^{e_{i,j}}\left(\frac{w}{p}, \frac{w}{p}\right) = 0 \quad (3-22)$$

where

$$K^{e_{i,j}}\left(\frac{w}{p}, \frac{w}{p}\right) = \iint (\rho \bar{V} \cdot \nabla N_i) (\rho \bar{V} \cdot \nabla N_j) dx dy. \quad (3-23)$$

Next, the local stiffness matrix for the pressure equation is

$$K^{e_{i,j}}(P, P) = f^e_i(P) \quad (3-24)$$

where

$$K^{e_{i,j}}(P, P) = \iint (\nabla N_i) \cdot (\nabla N_j) dx dy \quad (3-25)$$

$$f^e_i(P) = -\iint (\nabla N_i) \cdot (\rho \bar{V} \cdot \bar{V}) dx dy. \quad (3-26)$$

and for pressure functional equation,

$$K^{e_{i,j}}(Q, Q) = f^e_{i1}(Q) + f^e_{i2}(Q) \quad (3-27)$$

where

$$K_{i,j}^e(Q,Q) = \iint (\rho \bar{V} \cdot \nabla N_i) (\bar{V} \cdot \nabla N_j) dx dy \quad (3-28)$$

$$f_{i1}^e(Q) = - \iint (\nabla \rho)^2 \bar{V} \cdot \nabla N_i dx dy \\ - \iint N_i \rho \bar{V} (\bar{V} \cdot \nabla) \rho \bar{V} dx dy \quad (3-29)$$

$$f_{i2}^e(Q) = \int_{\Gamma} N_i \rho (\rho V^2 + P) V_n ds. \quad (3-30)$$

For three dimensional axisymmetric flows, the velocity components are defined by

$$\rho u = \frac{1}{r} \frac{\partial \psi}{\partial r} \quad (3-31)$$

and

$$\rho v = - \frac{1}{r} \frac{\partial \psi}{\partial x}. \quad (3-32)$$

The vorticity transport equation becomes

$$\frac{D(\omega/\rho)}{Dt} = \frac{\omega}{\rho} \frac{v}{r}. \quad (3-33)$$

Here, ω/ρ is no longer constant along a stream line. This leads to another equation governing three dimensional flows

with axial symmetry. That is,

$$\frac{D(\omega/pr)}{Dt} = 0. \quad (3-34)$$

This equation states that for three dimensional axisymmetric flows, $\omega/(pr)$ is conserved along a stream line.

The stream function equation in this case has the form

$$\nabla \cdot \left(\frac{1}{\rho r} \nabla \psi \right) + \omega = 0. \quad (3-35)$$

Thus, the finite element weighted residual formulation for these equations takes a similar form to that of the two dimensional flow case.

3.4 Solution procedure

To obtain solutions of the steady-state nonlinear partial differential equations shown in the above section, a relaxation procedure is applied. This relaxation procedure shown below is very efficient and is shown to be an excellent solver for nonlinear systems.

Assume we are at the n th iteration of the relaxation 'do-loop', and the n th solution of the dependent variable G^n is obtained from the system. The system matrix A^{n+1} is formed with G^n . Thus, we have

$$A^{n+1}G^n - F^{n+1} = R^{n+1} \quad (3-36)$$

where F^{n+1} is the right hand side of the matrix system and R^{n+1} is the residual of the system. When we get the solution of the dependent variable G^{n+1} , the matrix system will give an exact solution under A^{n+1} and F^{n+1} . Thus,

$$A^{n+1}G^{n+1} - F^{n+1} = 0 \quad (3-37)$$

and so a relationship between the increase of δG^{n+1} and the residual R^{n+1} is obtained, which is

$$A^{n+1}\delta G^{n+1} = -R^{n+1}. \quad (3-38)$$

To relax the system, a relaxation factor α is introduced. Thus,

$$A^{n+1} \delta G^{n+1} = -\alpha R^{n+1} \quad (3-39)$$

This relaxation method can be used for both the simultaneous solution procedure and the separate solution procedure of the stream function-vorticity-pressure functional formulation. The relaxation can also be applied to the stream function equation alone while other equations are being solved without relaxation. The relaxation factor is greater than one for over relaxation and less than one for under relaxation.

During each iteration, the stream function equation and vorticity transport equation or stream function equation alone are solved first, depending on whether the first order vorticity transport equation or the second order one is used. Then, pressure is calculated by solving the pressure equation or the pressure functional equation for subsonic flow. For transonic flow, the pressure functional equation is solved. Finally, the density is obtained from the energy equation. For transonic flows, the formulation requires the use of a artificial viscosity,³⁰ The form of the artificial viscosity used is

$$\bar{\rho} = \rho - \text{Max}(0, 1 - 1/M_i^2, 1 - 1/M_{i-1}^2) \rho_s \Delta s$$

where s is the stream line coordinate, $i-1$ is the upstream location of the element i , M is the Mach number, and ρ is density.

3.5 Boundary conditions

One of the advantages of the finite element stream function and vorticity formulation is that boundary conditions are simple to implement. In this work, three types of boundary conditions are studied. They are stream line boundaries, inlet and outlet boundaries, and free stream boundaries. Stream line boundaries are associated with body boundaries in inviscid flows and boundaries for symmetry. Inlet and outlet boundaries are needed for internal flow situations, such as, the nozzle flow and the channel flow. Free stream boundaries refer to the far-field boundaries for external flows.

Centre lines of the nozzle and the channel are considered stream lines because of symmetry. Thus, stream function boundary conditions have a very simple form along these lines. Stream function is also a constant along the upper wall of the nozzle and the channel. This constant must be determined by the inlet flow rate.

Pressure and pressure functional boundary conditions along a stream line are not required because the boundary integrals, appearing in the weighted residual finite element equations, vanish along a stream line.

A detailed discussion of boundary conditions for a particular flow problem is shown in the next chapter.

CHAPTER 4

SOLUTION EXAMPLES

CHAPTER 4.

SOLUTION EXAMPLES

In Chapter two, we derived the stream function-vorticity-pressure functional form of the steady Euler equations. In Chapter three, we applied the finite element method to these equations and derived their discretized form. In this Chapter, these steady equations are solved for both internal and external flows. The numerical solutions are compared with both analytical results and experimental data. Based on the numerical results and the vorticity transport equation, general vorticity conservation for inviscid flows is also discussed.

4.1 An introductory discussion.

Rotational effects in inviscid flows are mainly caused by upstream vorticity, because the Euler equations conserve it. An example is the incompressible inviscid flow in a channel with a sudden enlargement as shown in Figure 1. For irrotational flows, no vortex can be found in the channel. On the other hand, if the flow at the channel inlet is rotational, a vortex may be found at the corner of the sudden enlargement, as shown in Figure 2.

Nevertheless, not all problems can be adequately described by inviscid models. An example is the attached flow past a lifting airfoil. In the absence of viscosity, the velocity of the flow at the trailing edge is infinite and zero lift is predicted. In this situation, the irrotational assumption fails. However, because of mathematical simplicity of the irrotational model, it is still used for calculations of the lifting airfoil. To employ the irrotational model, an extraneous condition is needed at the trailing edge of the airfoil. This is the Kutta-Joukowski condition, which requires that the flow leave the airfoil smoothly at the trailing edge. Thus, the Kutta-Joukowski condition adds vorticity around the airfoil. The irrotational assumption conflicts with this condition. Possibly this is the reason that the full potential equation does not predict unique solutions. On the other hand, the

Euler equations can give reasonable solutions for the lifting case because of the conservative nature of the vorticity as explained by the vorticity transport equation.

It is believed that shock waves can also introduce vorticity into the flow, but only across shock waves.⁵⁰ In this study, it is shown that vorticity introduced after shock waves will be carried infinitely downstream because there is no vorticity dissipation in inviscid flows governed by the Euler equations. In fact, for rotational flows, although vorticity increases across the shock the increase is constrained because the ratio of vorticity to density remains constant, while the density increases. For irrotational flows, vorticity is not introduced across the shock in this study.

Finally, upstream vorticity can be caused by viscous properties of real flows.⁶⁷ In this case, as the vorticity transport equation shows, vorticity must be given at the upstream boundary in order to carry out a numerical solution. In addition, upstream supplies of heat can change the stagnation properties of the flow and so generate upstream vorticity. However, since flow problems with heat conduction are related to viscous properties of real fluids, numerical solutions for this kind of flows can be obtained from the full Navier-Stokes equations.

In the examples that follow, we focus on two inviscid flows, the flow in the internal nozzle and the flow over two dimensional airfoils.

4.2 Quasi-one dimensional nozzle flow

Quasi-one dimensional subsonic and transonic flows through nozzles are very important topics in fluid dynamics. Since analytical solutions are available, numerical solutions can be validated by comparing them with analytical solutions. The solutions can also apply to for two dimensional flows where comparisons can also be made with the quasi-one dimensional analytical solutions.

The numerical procedure used in this study for transonic quasi-one dimensional does not need the artificial density required for the standard solution procedure of the full functional equation. Thus, numerical results of this procedure can be made arbitrarily close to those from analytical models.

Since the flow is irrotational, the quasi-one dimensional nozzle flow can be solved using the potential equation. The first basic equation needed is the continuity equation,

$$\frac{d}{dx}(A\rho\frac{d\phi}{dx}) = 0 \quad (4-1)$$

where A is area, ρ is density, ϕ is velocity functional and x is the streamline coordinate. The density-velocity

relation is also needed for updating the density and pressure. That is,

$$\rho/\rho_0 = (1 - (\gamma - 1)u^2 / (2a_0^2))^{1/(\gamma - 1)} \quad (4-2)$$

where $\gamma = c_p/c_v$, a is the sound velocity and the '0' subscript equals stagnation properties.

The standard solution procedure is an iterative one. It solves the continuity equation for ϕ with an updating value of ρ . With this method, the solution for a subsonic flow is the same as the analytical solution. However, for transonic flows, artificial viscosity is needed for the convergence of the iterative procedure. Artificial viscosity introduced into a flow makes the choking point move upstream of the throat. In our study, we define a new relation for the full functional by using

$$\frac{dG}{dx} = \rho \frac{d\phi}{dx} \quad (4-3)$$

Thus, equation (4-1) becomes

$$\frac{d}{dx}(A \frac{dG}{dx}) = 0. \quad (4-4)$$

The variational principle for this equation does not require an iterative procedure. Thus, the product of the density

and the velocity can be determined by solving equation (4-4) only once. Coupled with the density-velocity relation, equation (4-2), density and velocity are determined.

The solution is unique for subsonic flows. However, for transonic flows this is not the case because expansion shocks may appear. Artificial viscosity or density are not needed because there are no iterations in the solution procedure. Nevertheless, the entropy condition must be satisfied or a physically meaningless expansion shock could be found.

The results of a quasi-one dimensional solution procedure are shown in Figure 3 and 4. Figure 3 shows the Mach number distribution along a nozzle that extends from $x=0$ to $x=10$ with the throat located at $x=5$. The area ratio of the nozzle inlet to the throat is 2.5 and the area ratio of the nozzle exit to the throat is 1.5. The flow problems are solved with five inlet Mach numbers of values 0.15, 0.18, 0.2, 0.22, 0.24. The figure shows that in all cases, numerical results of equation (4-4) agree very well with analytical and full functional solutions. Figure 4 shows pressure distributions along the nozzle for the same coordinates and Mach numbers as shown in Figure 3. Good agreement between pressure values can be seen. In order to see the comparison between the analytical solution and the numerical solution in detail, results are also given in

Table 1. Numerical solutions show that for subsonic flows, both the classical method and our method agree with the analytical solution.

For transonic flows, Mach number and pressure distributions along the nozzle are given in Figure 5 and Figure 6 for an inlet Mach number of 0.24. A detailed comparison is shown in Table 2. In Figure 5 and Figure 6, we see that the potential solution shifts the choking point upstream somewhere of the nozzle throat. The potential solution requires the artificial viscosity to obtain solutions and the results can vary with values of the artificial viscosity selected. However, the method shown in this work does not need artificial viscosity; a unique solution can be obtained with this method. The solution of equation (4-4) shows a good agreement with the analytical solution.

4.3 Two dimensional nozzle flow

In this study, the classical two dimensional and three dimensional axisymmetric internal nozzle flows are chosen as internal flow examples. The Euler equations are solved with the method developed in this study for subsonic and transonic flows for different inlet Mach numbers. Numerical solutions to these problems have been reported by Habashi and Hafez⁵³ and others.

A coarse grid for the two dimensional internal nozzle is given in Figure 7. The coarse grid has 8×30 nodes. A refined grid size also used has 8×100 nodes. The inlet area of the nozzle is 2.5 times bigger than the throat area. The exit area of the nozzle is 1.5 times bigger than the throat area.

Boundary conditions for these problems can be implemented easily. Along the centre line of the nozzle, the stream function value is chosen to be zero because the centre line can be considered a stream line. Along the upper wall, the stream function is also a constant determined by the inlet flow rate. Pressure and pressure functional boundary conditions along the nozzle centre line and the upper wall are not required because boundary integrals, appearing in the weighted residual finite element formulations, vanish along a stream line.

As shown in Chapter 3, to solve first order vorticity transport equation, vorticity boundary conditions along a stream line are determined by

$$\frac{\partial \epsilon}{\partial p} = \text{constant} \quad (4-5)$$

and for three dimensional axisymmetric flow, by

$$\frac{\epsilon}{rp} = \text{constant}. \quad (4-6)$$

If the second order vorticity transport equation is solved, vorticity boundary conditions along a stream line are not necessary, since the auxiliary boundary condition must be satisfied and the boundary integral disappears. However, vorticity boundary conditions at the inlet must be given.

Boundary conditions at the nozzle inlet are determined by the inlet flow situation. If an irrotational flow is expected, a uniform inlet velocity is given. If a rotational flow is going to be solved, a suitable curved velocity profile is assumed at the nozzle inlet. A typical curved velocity profile is given by the relation

$$u = a \cos(b \pi y) \quad (4-7)$$

where u is the inlet velocity, y is the transverse

coordinate of the flow field, and coefficients a and b are determined by matching the uniform inlet mass flow rate. At the inlet of the nozzle, the velocity in transverse direction is assumed to be zero. Stream function boundary conditions at inlet are determined by the inlet velocity profile. Vorticity and pressure boundary conditions at inlet are also determined by the inlet velocity profile.

Boundary conditions at inlet and outlet for the pressure functional for both subsonic and transonic flows are similar to velocity functional boundary conditions. At the outlet of the nozzle, pressure functional values are specified. At inlet, boundary integrals in the finite element formulations are carried out. For transonic flow problems, the iterative procedure is very similar to that of the transonic internal functional solution used by Habashi et al.⁶⁹ At the both inlet and outlet, pressure functional values must be specified. The increase of pressure functional values between inlet and outlet is determined by nozzle exit back pressure uniquely.

For internal nozzle flows, vorticity is given at the inlet through a velocity profile at inlet. Because vorticity is conserved for inviscid flows governed by the Euler equation, the upstream vorticity distribution is necessary.

Several inlet velocity profiles are shown in Figure 8. In this figure, the velocity ratio of u/U_0 where U_0 is the uniform velocity is plotted against transverse distance from the centre line. The irrotational limit of these velocity profiles is the uniform inlet flow. The coefficients "a" and "b" can be chosen the following way. Select "b" first and then calculate "a" from

$$m_{\text{uniform}} = \int_0^{y_0} \rho u dy \quad (4-8)$$

where y_0 is the nozzle inlet width and m_{uniform} is the mass flow rate of the uniform flow. The velocity profile values decrease from the centre line toward the nozzle wall.

Pressure values at the throat section are given for different inlet Mach numbers from 0.1 to 0.24 in Figure 9. As inlet Mach number increases, lower pressures are predicted. The pressure has a lowest value at the nozzle center because the flow is rotational.

Figure 10 shows stream line patterns drawn along the nozzle. For rotational flows, stream lines are spaced further apart as the distance from the center line increases. In comparison, for irrotational flows, stream lines are arranged uniformly.

When the stream function formulation is applied to internal transonic flow problems, it is very difficult to match the back pressure. If the pressure equation is employed, the back pressure can be used as a boundary condition for this formulation. However, sharp shocks cannot be calculated since shocks are smeared over many elements. The pressure functional formulation studied in this work, overcomes this difficulty.

The pressure functional formulation involves a similar approach to that for velocity functional for both subsonic and transonic flow problems. Boundary conditions are very simple to implement when finite element method is used. Along stream line boundaries, Neumann boundary conditions are satisfied since boundary integrals in finite element formulations are null. For transonic internal flows, pressure functional boundary conditions at inlet and outlet should be determined by the given back pressure. For a beginning guess, inlet and outlet boundary conditions can be chosen from the choking flow.

In Figure 11, the vorticity distribution along the nozzle boundary is shown. As the nozzle throat is approached, vorticity decreases because the density decreases. Across the shock wave, a sudden jump of the vorticity is observed for rotational flows. However, the ratio of vorticity to density is still a constant unless an

explicitly argued vorticity term exists. For rotational flows, Mach number distributions along the nozzle are shown in Figure 12 and Figure 13. The shock along the central line is stronger than the irrotational shock because the velocity reaches a higher value. Pressure distributions along the nozzle are shown in Figure 14 and 15. The irrotational functional solutions for the same back pressures are also shown in these figures. For lower back pressure, the shock is stronger as shown in Figure 13. The pressure reaches a lower value for a lower back pressure as shown in Figure 15.

The equal vorticity lines are shown in Figure 16 and 17. There are jumps for vorticity values across a shock. The stronger a shock, the bigger the jump in vorticity. For higher vorticity values, the equal vorticity lines end on the nozzle boundary because vorticity decreases in the converging part and increases in the diverging part of the nozzle.

4.4 External flows

The Euler equations are also solved for flows over the NACA-0012 airfoil, as external flow examples using the formulation developed in this work. Comparisons are made with experimental data.⁷⁵

Boundary conditions for external flows in these cases are discussed as follows. Free stream boundary conditions for stream function are

$$\psi = U_{\infty} \rho_{\infty} (y \cos \alpha - x \sin \alpha). \quad (4-9)$$

where U_{∞} is free stream velocity, ρ_{∞} is free stream density and α is attack angle of the airfoil. The free stream boundary condition given in Reference 57 is correct only for incompressible flows. For compressible flows, the error caused by the free stream boundary condition given in Reference 57 is up to twenty percent if free stream Mach number is 0.7. For higher free stream Mach number, higher errors are expected. If the pressure equation is solved, the free stream pressure value is taken to be the boundary condition for the pressure equation. Free stream boundary conditions for the pressure functional equation are similar to the free stream boundary conditions for the velocity functional equation.

Boundary conditions for the pressure functional can be written as

$$Q = P_{\infty}(x \cos\alpha + y \sin\alpha). \quad (4-10)$$

where P_{∞} is free stream pressure. The airfoil surface can be considered to be a stream line. Thus, the stream function is a constant along the airfoil. No boundary conditions are required for vorticity, pressure and pressure functional on the airfoil because boundary integrals appearing in finite element formulations for these variables vanish.

A coarse grid for flows over the NACA-0012 airfoil is shown in Figure 18. The refined grid is shown in Figure 19. The coarse grid has 21×118 nodes and the refined grid has 34×204 nodes. Numerical results for both the coarse grid and the refined grid are presented and compared. The presentation includes subsonic flows and supersonic flows for both nonlifting airfoil and lifting airfoil. The convergence rates of this solution procedure are also shown. Numerical results are compared with experimental data for both subsonic and transonic flows. These experimental data were designed for estimate of numerical solution procedures and were used by others.⁷⁵

For subsonic non-lifting flows, pressure coefficients on the airfoil are shown in Figure 20 and 21 for free stream Mach number 0.5 and 0.703. For supersonic non-lifting flows, pressure coefficients are shown in Figure 22 and 23 for free stream Mach number 0.803 and 0.829. In the non-lifting case, the Kutta condition is not needed because the flow is symmetric. Numerical results show that for subsonic flows, solutions of the steady Euler equations agree well with experimental data. For transonic flows, the pressure coefficient distribution curve moves further upstream.

Numerical results for the lifting airfoil are also presented in this work. Comparison with experimental results are made for both subsonic and transonic flows. In Figure 24, the pressure coefficient over the airfoil for free stream Mach number 0.502 and an angle of attack 2.06 is shown. The upper curve represents the pressure coefficients on the upper surface of the airfoil. For this free stream Mach number and attack angle, the flow is subsonic. The numerical solution is very close to experimental data. The pressure coefficients for free stream Mach number 0.75 with attack angles 2.0 and 3.0 are shown in Figure 25 and 26. These cases are transonic flows. For the lifting airfoil, the Kutta condition is implemented for the reason discussed above. Good agreement with experimental data appears.

The convergence history for free stream Mach number 0.703 over the NACA-0012 airfoil is shown in Figure 27. The convergence history for free stream Mach number 0.803 is shown in Figure 28. For subsonic flows, only ten iterations are needed. For transonic flows, the calculation needs more iterations to converge. Comparisons of numerical results between refined grid and unrefined grid are shown in Figure 29 and 30. For subsonic flows, the results are close to each other. However, for transonic flows, higher shock Mach number is obtained because the artificial viscosity has lower values. Good agreement shows that grid generations used in this work can predict accurate results.

CHAPTER 5

CONCLUDING REMARKS

CHAPTER 5.

CONCLUDING REMARKS

This study shows that the pressure functional formulation coupled with the stream function-vorticity method is a very useful approach in numerical solution of the steady Euler equations. In particular, the difficulty encountered when the stream function formulation is used for internal transonic flows is overcome easily by using the pressure functional approach. Next, the study of the vorticity transport equation in this work completes the detailed formulation of the stream function-vorticity method for compressible inviscid flow problems. This makes it possible to use this formulation to solve the steady Euler equations for transonic flow problems.

5.1 Pressure functional method

Transonic internal nozzle flows had been difficult to solve with stream function formulations. This is because matching the nozzle back pressure is difficult when stream function formulation is applied. Furthermore, when the pressure equation is coupled with the stream function formulation, the back pressure of the nozzle can be used as a boundary condition. However, no sharp shock can be found; the shock is smeared over many elements.

On the other hand, in this study, a new formulation is proposed based on a new variable definition. This variable is called pressure functional. If this new formulation is used to solve internal transonic flows, the difficulty encountered for the stream function formulation is overcome easily. We have shown that this formulation is easy to handle. The partial differential equation relating this variable to variables of the flow field is derived from the momentum equation. Also, boundary conditions for the pressure functional equation are very simple to implement when finite element weighted residual approach is applied, since along stream lines, boundary integrals appearing in the finite element formulation are null. Inlet and outlet boundary conditions are very similar to those of the velocity potential method. For external flows, free stream boundary conditions also take similar forms.

This solution procedure for internal transonic flows is very similar to that for the velocity potential equation. Pressure functional values at both inlet and outlet must be specified. Finally, the increase of the pressure functional values between inlet and outlet is uniquely determined by the nozzle exit back pressure.

5.2 Stream function-vorticity formulation

Prior to this work, the stream function-vorticity method was mainly applied to incompressible flow problems. For compressible inviscid flows, the modified stream function formulation was employed to take account of rotational effects. The modified stream function formulation requires knowledge of the vorticity. Unfortunately, vorticity is not tracked if the vorticity transport equation is not involved.

This derivation of the vorticity transport equation for compressible inviscid fluid flows is valid for non-heat conducting flow of perfect gases. In most aerodynamic problems of interest, this is a reasonable assumption.

We have successfully applied our stream function-vorticity formulation of the Euler equations to a variety of fluid flows of engineering interests.

5.3 Conservation of vorticity

Our expression for the vorticity transport equation indicates that vorticity is conserved in inviscid flows. Thus, vorticity can be initiated upstream to create rotational flows. This is the case in the internal nozzle flow example studied in this work. Because the real flow is viscous, the inlet flow for the nozzle could be rotational. We gave this inlet rotational condition as a non-uniform inlet velocity profile.

Nevertheless, in some cases, the Euler equations cannot predict a physical flow problem correctly. An example is the solution of the Euler equations for the flow past a lifting airfoil. In this case, the mathematical model is not valid because the free stream flow is irrotational. According to the vorticity transport equation, the flow through the entire field is irrotational because the vorticity is conserved in the inviscid fluid flow governed by the Euler equations. In this situation, the irrotational assumption fails.

In order to get a solution which is physically correct, an extraneous condition is needed at the trailing edge of the airfoil. This condition is the famous Kutta-Joukowski condition. The Kutta condition forces the flow to leave the airfoil smoothly. Thus, the Kutta condition introduces

vorticity around the airfoil. However, the Kutta condition is implemented, it conflicts with the irrotational full potential model because of the irrotational assumption. Possibly this is the reason that the full potential equation predicts non-unique solutions.

5.4 Solution technique

The vorticity transport equation studied in this work is a first order partial differential equation. It is very difficult to solve such first order partial differential equations directly with either the finite element method or the finite difference method. The finite element weighted residual formulation leads to a singular matrix as the central finite difference approach does.

In this study, the vorticity transport equation is solved by two procedures. The first approach is to solve the vorticity transport equation simultaneously with the stream function equation. In this procedure, the vorticity transport equation takes a first order form. The weighted residual finite element formulation is used for both the stream function equation and the vorticity transport equation. Because these two equations are solved simultaneously, the resulting matrix is not singular.

The second procedure to solve the vorticity transport equation is to derive the second order form of this equation and then apply the finite element weighted residual approach to the resulting equation. In this case, the stream function equation and the vorticity equation can be solved independently. However, an auxiliary boundary condition must be satisfied as the compensation for the increase of

the partial differential equation order. In this work, it is shown that the auxiliary boundary condition is very simple to implement with the finite element method; the boundary integral appearing in the finite element formulations vanishes.

5.5 Numerical results

Numerical results for inviscid flow problems in this work are discussed in previous chapters. For the two dimensional nozzle, numerical results are compared with the solutions of the full potential equation. Good agreement among them shows that approaches proposed in this study are efficient and useful. For transonic flows, the nozzle is choked upstream somewhere of the throat. Further studies of the quasi-one dimensional transonic nozzle flow point out that choking upstream of the throat is caused by the artificial viscosity. For the NACA-0012 airfoil, numerical results are compared with experimental data and results of the full potential equation. Good agreement shows the solution approaches proposed in this study are also useful for external flows.

5.6 Final comments

This thesis demonstrates that the Euler equations can be solved with the stream function-vorticity-pressure functional formulation, provided the vorticity transport equation is employed. With the pressure functional, the difficulty encountered in the transonic internal stream function solutions is overcome. The finite element method can be used to perform the numerical calculations. The approach is useful for both subsonic and transonic flows.

REFERENCES

REFERENCES

1. John, J.E.A., *Gas Dynamics*, Allyn and Bacon, Inc. Boston, Massachusetts, 1984.
2. Turner, M., Clough, R., Martin, H., Topp, L. "Stiffness and Deflection Analysis of Complex Structure," *J. Aero. Sci.*, Vol. 23, No. 9, 1956, pp. 805-823.
3. Clough, R. W., "The Finite Element Method in Plane Stress Analysis," *Proc. 2nd Conf. Electronic Computation*, American Society of Civil Engineers, Pittsburgh, Pennsylvania, 1960, pp. 345-378.
4. Argyris, J.H., *Recent Advances in Matrix Methods of Structural Analysis*, Pergamon, Elmsford, N.Y., 1963.
5. Zienkiewicz, O.C., Cheung, Y.K., "Finite Elements in the Solution of Field Problems," *The Engineer*, 1965, pp. 507-510.
6. Oden, J.T., *Finite Elements of Nonlinear Continua*, McGraw-Hill, New York, 1972.
7. Babuska, I., Aziz, A.K. "Lectures on the Mathematical Foundations of the Finite Element Method," *Mathematical Foundations of the Finite Element Method with*

Applications to Partial Differential Equations, Academic, New York, 1972, pp. 1-345.

8. Ciarlet, P.G., Raviart, P.A., "General Lagrange and Hermite Interpolation in R^n with Applications to the Finite Element Method," *Arch. Rat. Mech. Anal.*, Vol. 46, 1972, pp. 177-199.

9. Aubin, J.P. *Approximation of Elliptic Boundary Value Problems*, Wiley-Interscience, New York, 1972.

10. Strang, G., Fix, G.J., *An Analysis of the Finite Element Method*, Prentice Hall, Englewood Cliffs, New Jersey, 1973.

11. Lions, J.L., Magenes, E., "Non-Homogeneous Boundary-Value Problems and Applications," Vol. I (Trans. From 1963 French Edition by P. Kenneth), Springer-Verlag, 1972.

12. Cheng, R.T., "Numerical Solution of the Navier-Stokes Equations by the Finite Element Method," *Physics of Fluids*, Vol. 15, No. 12, 1972, pp. 2093-2105.

13. Chan, S.T., Larock, B.E., "Potential Flow around A Cylinder between Parallel Walls by Finite Element Methods," *J. Engng. Mech. Div., ASCE*, Vol. 98, No. EM 5, 1972, pp. 1317-1322.

14. Baker, A.J. "Finite Element Solution Algorithm for Viscous Incompressible Fluid Dynamics," *Int. J. Num. Meth. Eng.*, Vol. 6, 1973, pp. 89-101.
15. Olson, M.E. "Formulation of a Variational Principle-Finite Element Method for Viscous Flows," *Proc. Variational Meth., Eng.*, Southampton University, 1972, pp. 5.27-5.38.
16. Chung, T.J., *Finite Element Analysis in Fluid Dynamics*, McGraw-Hill International Book Company, New York, 1978.
17. Baker, A.J., *Finite Element Computational Fluid Mechanics*, McGraw-Hill International Book Company, New York, 1983.
18. Salas, M.D., "Foundations for the Numerical Solution of the Euler Equations," *Advances in Computational Transonic*, Ed. W.G. Habashi, Swansea, U.K., 1985, pp. 343-369.
19. Murman, E.M., Cole, J.D., "Calculation of Plane Steady Transonic Flows," *AIAA J.*, Vol. 9, No. 1, 1971, pp. 114-121.
20. South, J.C., "A Historical Perspective and Overview of Computational Transonics," *Advances in Computational Transonic*, Ed. W.G. Habashi, Swansea, U.K., 1985, pp.

1-20.

21. Jameson, A., "Transonic Potential Calculations Using Conservation Form," *Proceedings of the AIAA 2nd Computational Fluid Dynamics Conference, Hartford, Connecticut, 1975*, pp. 148-155.


22. Hafez, M.M., South, J.C., Murman, E.M., "Artificial Compressibility Methods for Numerical Solution of Transonic Full Potential Equation," *AIAA J.*, Vol. 17, No. 8, 1979, pp. 838-844.

23. Holst, T.L., Ballhaus, W.F., "Fast Conservative Schemes for the Full Potential Equation Applied to Transonic Flows," *AIAA J.*, Vol. 17, No. 2, 1979, pp. 145-152.

24. Purvis, J.W., Burkhalter, J.E., "Prediction of Critical Mach Number for Store Configurations," *AIAA J.*, Vol. 17, No. 11, 1979, pp. 1170-1177.

25. Doctors, L.J., "An Application of the Finite Element Technique to Boundary Value Problems of Potential Flow," *Int. J. Num. Meth. Engng*, Vol. 2, 1970, pp. 243-252.

26. Norrie, D.H., Vries, G. De, "The Application of the Finite Element Technique to Potential Flow Problems," *J. Applied Mechanics*, 1971, 798-802.



27. Deconinck, H., Hirsch, C., "Subsonic and Transonic Computation of Cascade Flows," *Computing Methods in Applied Sciences and Engineering*, North-Holland, Amsterdam, 1980, pp. 175-195.

28. Bristeau, M.O., Glowinski, R., Periaux, J., Perrier, P., Pironneau, O., Poirier, G., "Applications of Optimal Control and Finite Element Methods to the Calculation of Transonic Flows and Incompressible Viscous Flows," *Numerical Methods in Applied Fluid Dynamics*, Academic Press, London, 1980, pp. 203-312.

29. Eberle, A., "Finite Element Methods for the Solution of the Full Potential Equation in Transonic Steady and Unsteady Flow," *Finite Elements in Fluids*, Vol. 4, Wiley, Chichester, 1982, pp. 483-504.

30. Habashi, W.G., Hafez, M.M., "Finite Element Solutions of Transonic Flow Problems," *AIAA J.*, Vol. 20, No. 10, 1982, pp. 1368-1376.

31. Habashi, W.G., Hafez, M.M., "Finite Element Stream Function Solutions for Transonic Turbomachinery Flows," *AIAA Paper*, No. 82-1268, 1982.

32. Hafez, M.M., Lovell, D., "Numerical Solution of Transonic Stream Function Equation," *AIAA J.*, Vol. 21, No. 3, 1983, pp. 327-335.

33. Deconinck, H., Hirsch, CH., "Finite Element Methods for Transonic Blade-to-Blade Calculation in Turbomachines," *ASME Journal of Engg. For Power*, Vol. 103, 1981, pp. 665-677.
34. Steger, J.L., Pulliam, T.H., Chima, R.V., "An Implicit Finite Difference Code for Inviscid and Viscous Cascade Flow," *AIAA Paper*, 80-1427, 1980.
35. Keck, H., Haas, W., "Finite Element Analysis of Quasi-Three Dimensional Flow in Turbomachines," *Finite Elements in Fluids*, Vol. 4, John Wiley Sons Ltd, 1982, pp. 531-550.
36. Habashi, W.G., Youngson, G.G., "A Transonic Quasi-3D Analysis for Gas Turbine Engines Including Split-Flow Capability for Turbofans," *International Journal for Numerical Methods in Fluids*, Vol. 3, 1983, pp. 1-21.
37. Cedar, R.D., Stow, P., "The Addition of Quasi-Three-dimensional Terms into a Finite Element Method for Transonic Turbomachinery Blade-to-Blade Flows," *International Journal for Numerical Methods in Fluids*, Vol. 5, 1985, pp. 101-114.
38. Salas, M., Jameson, A., Melnik, R., "A Comparative Study of the Nonuniqueness Problem of the Potential

Equation," AIAA Paper, No. 83-1888, 1983.

39. Jameson, A., Schmidt, W., Turkel, E., "Numerical Solutions for the Euler Equations by Finite Volume Methods Using Runge Kutta Time Stepping Schemes," AIAA Paper, No. 81-1259, 1981.

40. Buning, P.G., Steger, J.L., "Solution of the Two-Dimensional Euler Equations with Generalized Coordinate Transformation Using Flux Vector Splitting," AIAA Paper, No. 82-0971, 1982.

41. Johnson, G.M., "An Alternative Approach to the Numerical Simulation of Steady Inviscid Flow," *Proceedings of the Seventh International Conference on Numerical Methods in Fluid Dynamics*, Lecture Notes in Physics, Vol. 141, Ed. Reynolds, W.C. And MacCormack, R.W., Springer-Verlag, 1981.

42. Pulliam, T., Jespersen, D., Childs, R., "An Enhanced Version of an Implicit Code for the Euler Equations," AIAA Paper No. 83-0344, 1983.

43. Steinhoff, J., Jameson, A., "Multiple Solutions for the Transonic Potential Flow Past an Airfoil," AIAA J., Vol. 20, No. 11, 1982, pp. 1521-1525.

44. Johnson, G.M., "Relaxation Solution of the Full Euler Equations," *Proceedings of the Eighth International*

Conference on Numerical Methods in Fluid Dynamics, Lecture Notes in Physics, Vol. 170, Ed. Krause, E., Springer-Verlag, 1982.

45. Jespersen, D.C., "A Multigrid Method for the Euler Equations," *AIAA Paper*, No. 83-0124, 1983.

46. Rizzi, A., Skolleremo, G., "Semidirect Solution to Steady Transonic Flow by Newton's Method," *Proceedings of the Seventh International Conference on Numerical Methods in Fluid Dynamics*, Lecture Notes in Physics, Vol. 141, Ed. Reynolds, W.C. And MacCormack, R.W., Springer-Verlag, 1981.

47. Bruneau, C.H., Chattot, J.J., Laminie, J., Guiu-Roux, J., "Finite Element Least Square Method for Solving Full Steady Euler Equations in a Plane Nozzle," *Proceedings of the Eighth International Conference on Numerical Methods in Fluid Dynamics*, Lecture Notes in Physics, Vol. 170, Ed. Krause, E., Springer-Verlag, 1982.

48. Shen, H.-L., Kee, M.-K., Dong, Q.-T., Li, N., "Time-Dependent Sweep Finite Element Analysis of Transonic Flow," *Finite Elements in Fluids*, Vol. 5, Ed. Gallagher, R.H., John Wiley Sons Limited, 1984.

49. Ecer, A., Akay, H.U., "A Finite Element Formulation for Steady Transonic Euler Equations," *AIAA Journal*, Vol. 21, No. 3, 1983, pp. 343-350.

50. Akay, H.U., Ecer, A., "Application of a Finite Element Algorithm to the Solution of Steady Transonic Euler Equations," *AIAA Journal*, Vol. 21, No. 11, 1983, pp. 1518-1524.

51. Steger, J.L.; Warming, R.F., "Flux Vector Splitting of the Inviscid Gas Dynamics Equations with Application to Finite Difference Methods," NASA TM-78605, 1979.

52. Johnson, G.M., "Accelerated Solution of the Steady Euler Equations," *Advances in Computational Transonic*, Ed. W.G. Habashi, Swansea, U.K., 1985, pp. 473-501.

53. Habashi, W.G., Hafez, M.M., "Finite Element Solutions of Inviscid Transonic External and Internal Flows," *Advances in Computational Transonic*, Ed. W.G. Habashi, Swansea, U.K., 1985, pp. 671-701.

54. Hafez, M.M., Habashi, W.G., Kotiuga, P.L., "Conservative Calculations of Non-Isentropic Transonic Flows," *International Journal for Numerical Methods in Fluids*, Vol. 5, 1985, pp. 1047-1057.

55. Sherif, A., Hafez, M.M., "Computation of Three Dimensional Transonic Flows Using Two Stream Functions," *AIAA Paper*, No. 83-1948, 1983.

56. Habashi, W.G., Hafez, M.M., "Finite Element Stream Function Solutions for Transonic Turbomachinery Flows,"

Journal of Numerical Methods for Partial Differential Equations, Vol. 1, No. 2, 1985, pp. 127-144.

57. Atkins, H.L., Hassan, H.A., "A New Stream Function Formulation for the Steady Euler Equations," *AIAA Journal*, Vol. 23, 1985, pp. 701-706.

58. Huang, C.-Y., Dulikravich, G.S., "Stream Function and Stream-Function-Coordinate (SFC) Formulation for Inviscid Flow Field Calculations," *Computer Methods in Applied Mechanics and Engineering*, Vol. 59, 1986, pp. 155-177.

59. Cheng, R.T., "Numerical Solution of the Navier-Stokes Equations by Finite Element Method," *Physics of Fluids*, Vol. 15, 1972, pp. 2098-2105.

60. Baker, A.J. "Finite Element Solution Algorithm for Viscous Incompressible Fluid Dynamics," *International Journal for Numerical Methods in Engineering*, Vol. 6, 1973, pp. 89-101.

61. Taylor, C., Hood, P., "A Numerical Solution of the Navier-Stokes Equations Using the Finite Element Technique," *Computers and Fluids*, Vol. 1, 1973, pp. 73-100.

62. Olson, M.D., Tuann, S.Y., "Primitive Variables versus Stream Function Finite Element Solutions of the Navier-Stokes Equations," *Finite Element Method in Flow*

Problems, S. Margherita Ligure, 1976, pp. 57-68.

63. Campion-Renson, A., Crochet, M.J., "On the stream Function-vorticity Finite Element Solutions of Navier-Stokes Equations," *International Journal for Numerical Methods in Engineering*, Vol. 12, 1978, pp. 1809-1818.

64. Comini, G., Del Giudice, S., Strada, M., "Finite Element Analysis of Laminar Flow in the Entrance Region of Ducts," *International Journal for Numerical Methods in Engineering*, Vol. 15, 1980, pp. 507-517.

65. Dhatt, G., Fomo, B.K., Bourque, C., "A Finite Element Formulation for the Navier-Stokes Equations," *International Journal for Numerical Methods in Engineering*, Vol. 17, 1981, pp. 199-212.

66. Mizukami, Akira, "A Stream Function-Vorticity Finite Element Formulation for Navier-Stokes Equations in Multi-Connected Domain," *International Journal for Numerical Methods in Engineering*, Vol. 19, 1983, pp. 1403-1420.

67. Fang, Z., Saber, A.J., "Marching Control Volume Finite Element Calculation for Developing Entrance Flow," *AIAA Journal*, Vol. 25, 1987, pp. 346-348.

68. Peeters, M.F., Habashi, W.G., Dueck, E.G., "Finite Element Stream Function-Vorticity Solutions of the

Incompressible Navier-Stokes Equations," *International Journal for Numerical Methods in Fluids*, Vol. 7, No. 1, 1987, pp. 17-27.

69. Habashi, W.G., Peeters, M.F., Guevremont, G., Hafez, M.M. "Finite-Element Solutions of the Compressible Navier-Stokes Equations," *AIAA Journal*, Vol. 25, No. 7, 1987, pp. 944-948.

70. Habashi, W.G., Hafez, M.M., Kotiuga, P.L., "Finite Element Methods for Internal Flow Calculations," *AIAA Paper*, No. 83-1404, 1983.

71. Owczarek, J.A., *Fundamentals of Gas Dynamics*, International Textbook Company, Scranton, Pennsylvania, 1968, pp. 43-47.

72. Owczarek, J.A., *Fundamentals of Gas Dynamics*, International Textbook Company, Scranton, Pennsylvania, 1968, pp. 69-70.

73. Moretti, G., "Numerical Analysis of Compressible Flow: An Introspective Survey," *AIAA Paper*, No. 79-1510, 1979.

74. Serrin, J., "Mathematical Principles of Classical Fluid Mechanics," *Encyclopedia of Physics*, edited by S. Flugge, Vol. VIII/1, *Fluid Dynamics I*, coedited by C. Truesdell, Springer-Verlag, Berlin, 1959, pp. 125-263.

75. Thibert, J.J., Grandjacques, M., Ohman, L.H., "NACA 0012 Airfoil, An Experimental Data Base for Computer Program Assessment," AGARD-AR-138, May 1979, pp. A1-1-A1-19.

76. Holst, T.L., Kaynak, U., Gundy, K.L., Thomas, S.D., Flores, J., Chaderjian, N.M., "Transonic Wing Flows Using an Euler/Navier-Stokes Zonal Approach," *J. Aircraft*, Vol. 24, No. 1, 1987, pp. 17-24.

TABLES AND FIGURES

Table 1. 1-D Nozzle Solution (choking)

Aera	Pressure Ratio P/P0		
	Analytical	This work	Potential
2.46985	0.95984	0.95984	0.95984
2.23967	0.95065	0.95066	0.95066
1.97949	0.93570	0.93575	0.93575
1.74992	0.91581	0.91587	0.91587
1.55096	0.88940	0.88946	0.88946
1.38261	0.85474	0.85479	0.85479
1.24487	0.81007	0.81014	0.81014
1.13774	0.75420	0.75430	0.75430
1.06122	0.68718	0.68723	0.68723
1.01530	0.61060	0.61072	0.61072
1.00000	0.52828	0.53222	0.53274
1.00510	0.57604	0.57630	0.57630
1.02041	0.62283	0.62296	0.62296
1.04591	0.66739	0.66748	0.66748
1.08162	0.70899	0.70908	0.70908
1.12754	0.74722	0.74723	0.74724
1.18365	0.78155	0.78163	0.78163
1.24997	0.81215	0.81219	0.81219
1.32650	0.83899	0.83902	0.83902
1.41322	0.86230	0.86232	0.86232
1.48995	0.87861	0.87862	0.87862

Table 2. 1-D Nozzle Solution (transonic)

Aera	Pressure Ratio P/P0		
	Analytical	This work	Potential
2.46985	0.95984	0.95984	0.95976
2.23967	0.95065	0.95066	0.95055
1.97949	0.93570	0.93575	0.93561
1.74992	0.91581	0.91587	0.91567
1.55096	0.88940	0.88946	0.88920
1.38261	0.85474	0.85479	0.85442
1.24487	0.81007	0.81014	0.80961
1.13774	0.75420	0.75430	0.75351
1.06122	0.68718	0.68723	0.68592
1.01530	0.61060	0.61072	0.60792
1.00000	0.52828	0.53222	0.51169
1.00510	0.47942	0.48005	0.42044
1.02041	0.43315	0.43277	0.60544
1.04591	0.65678	0.65684	0.65682
1.08162	0.70153	0.70158	0.70156
1.12754	0.74155	0.74159	0.74158
1.18365	0.77720	0.77723	0.77722
1.24997	0.80866	0.80869	0.80869
1.32650	0.83617	0.83619	0.83618
1.41322	0.85999	0.86000	0.86000
1.48995	0.87663	0.87663	0.87663

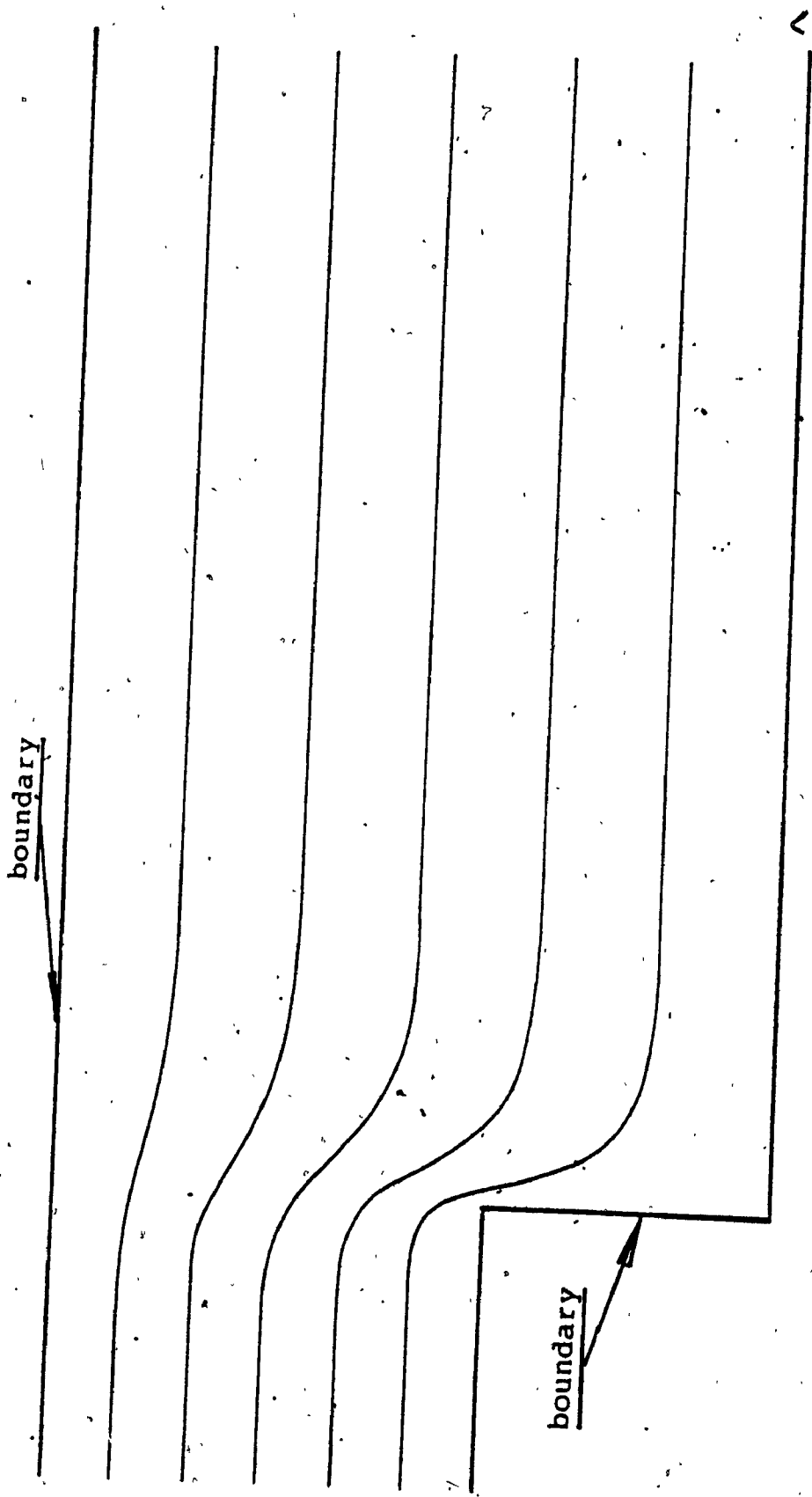


Fig. 1. Stream lines of irrotational flow

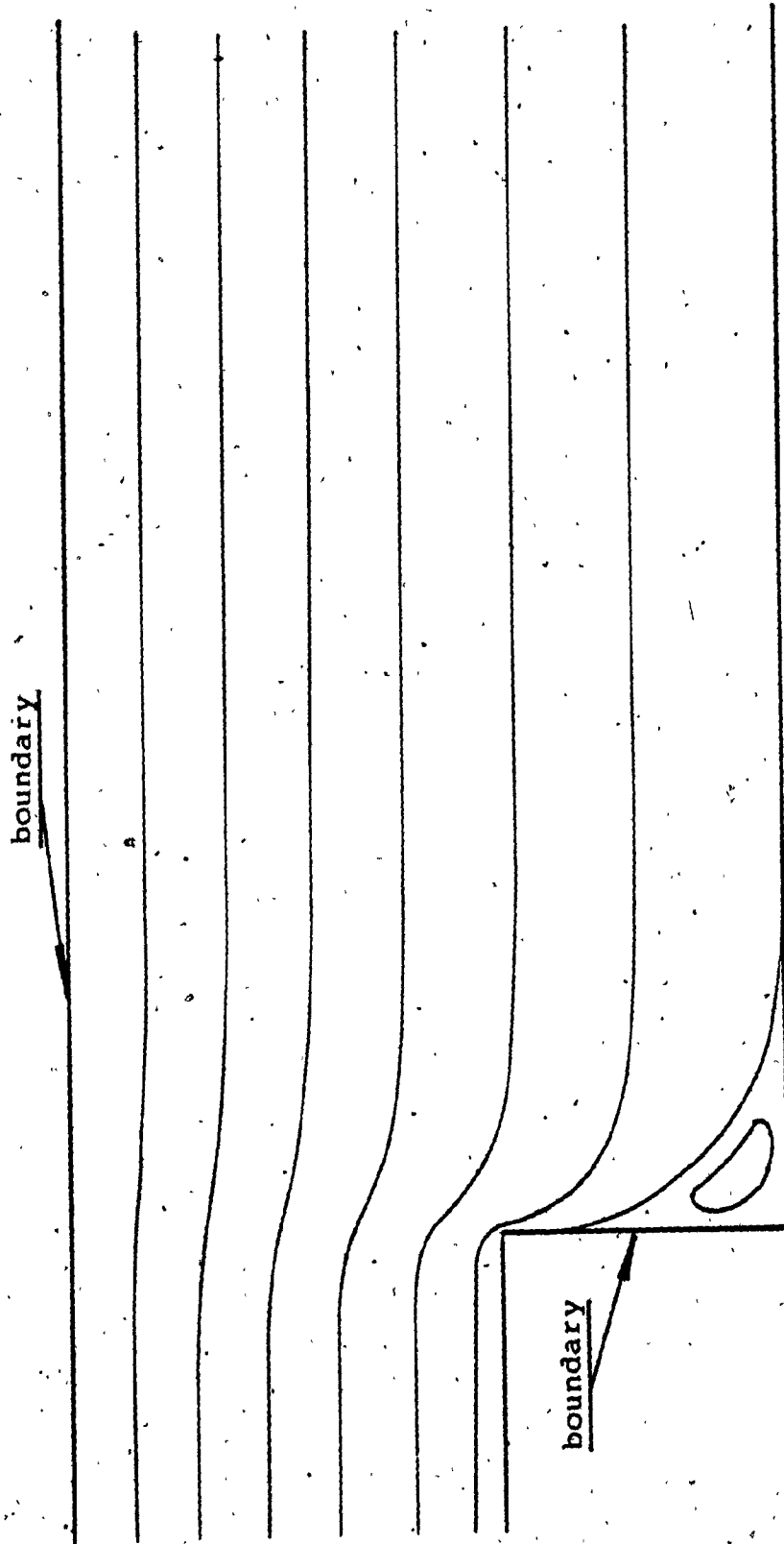


Fig. 2. Stream lines of rotational flow

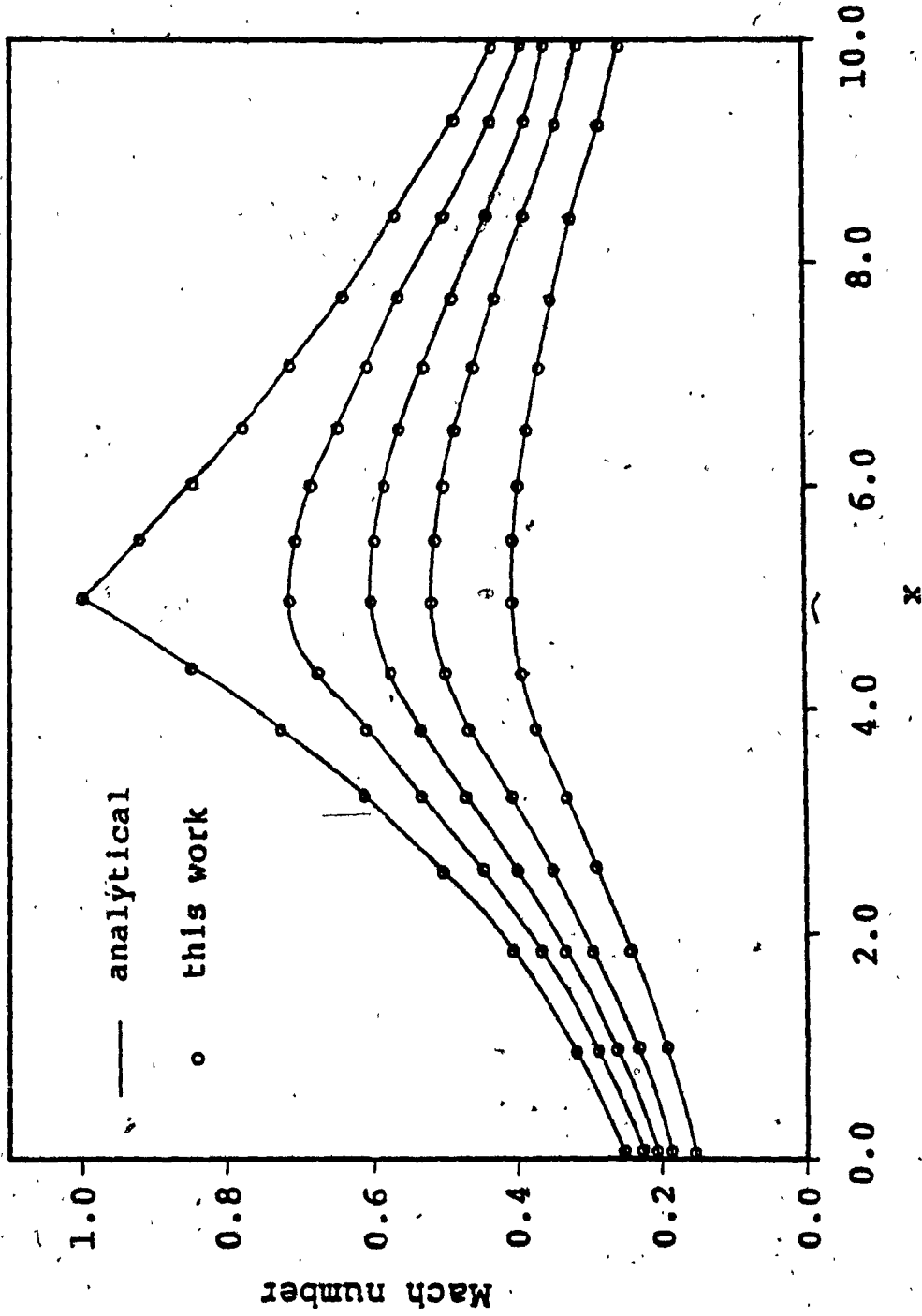


Fig. 3. Mach numbers along the nozzle

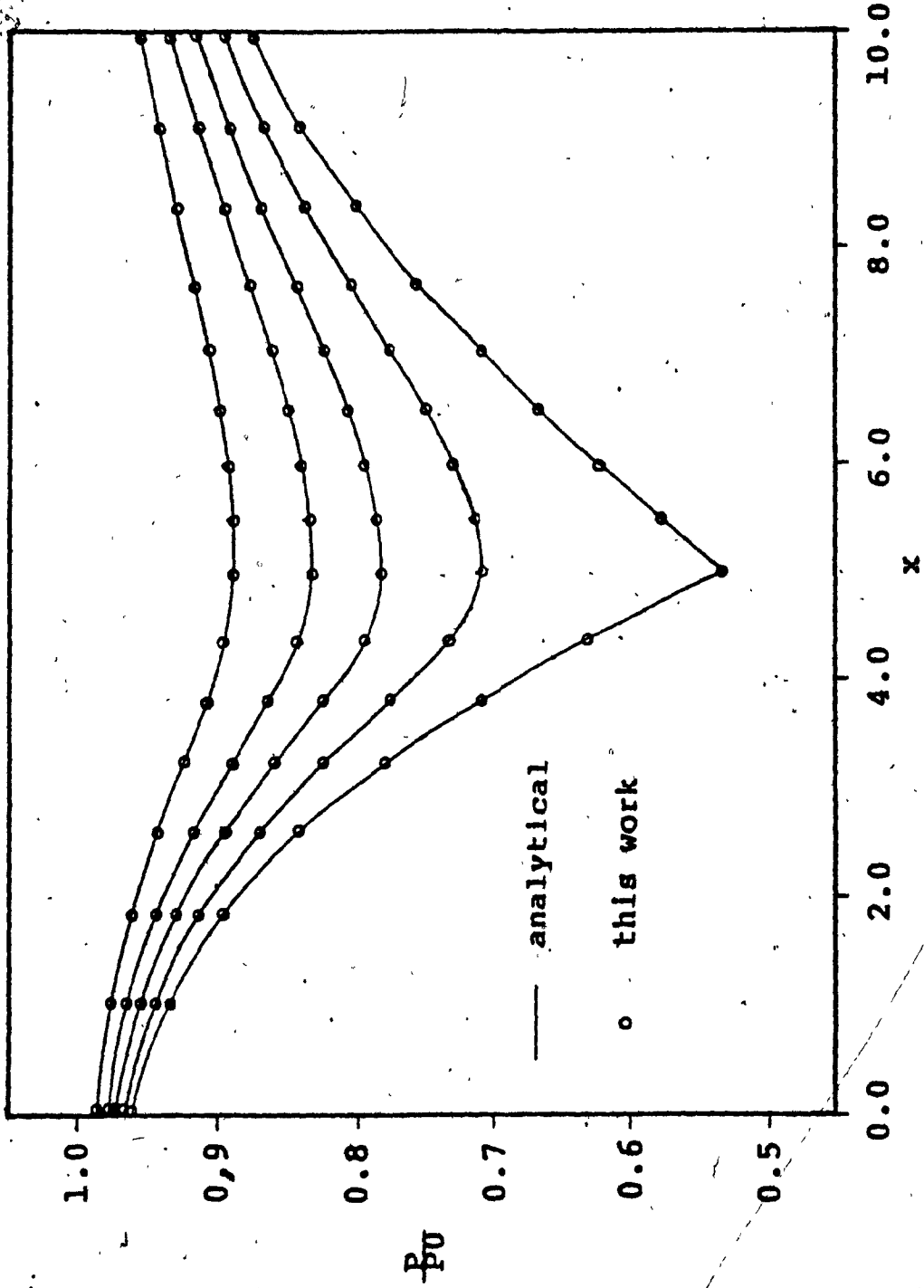


Fig. 4. Pressure distribution along the nozzle

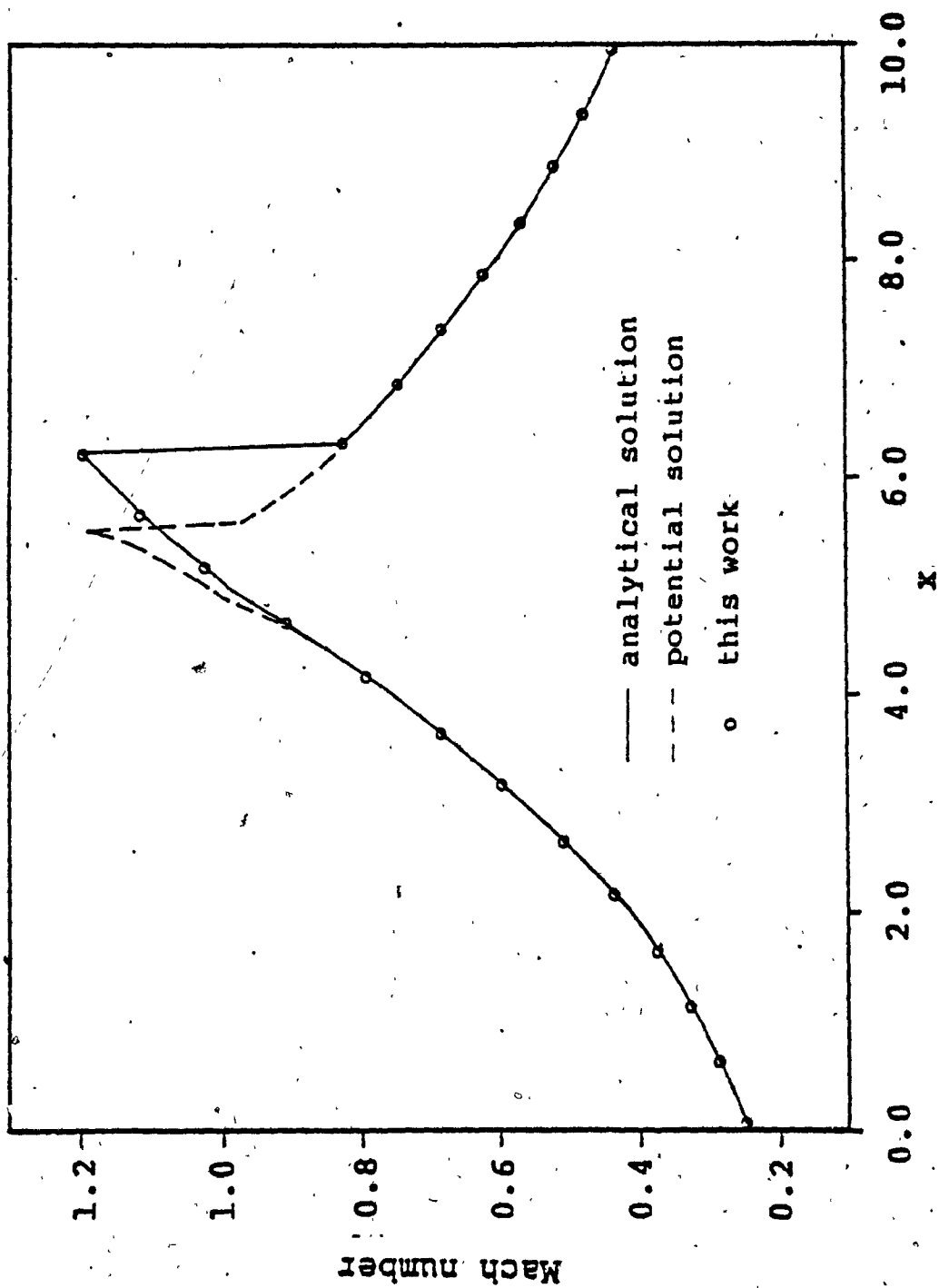


Fig. 5. Mach number along the nozzle for transonic flow

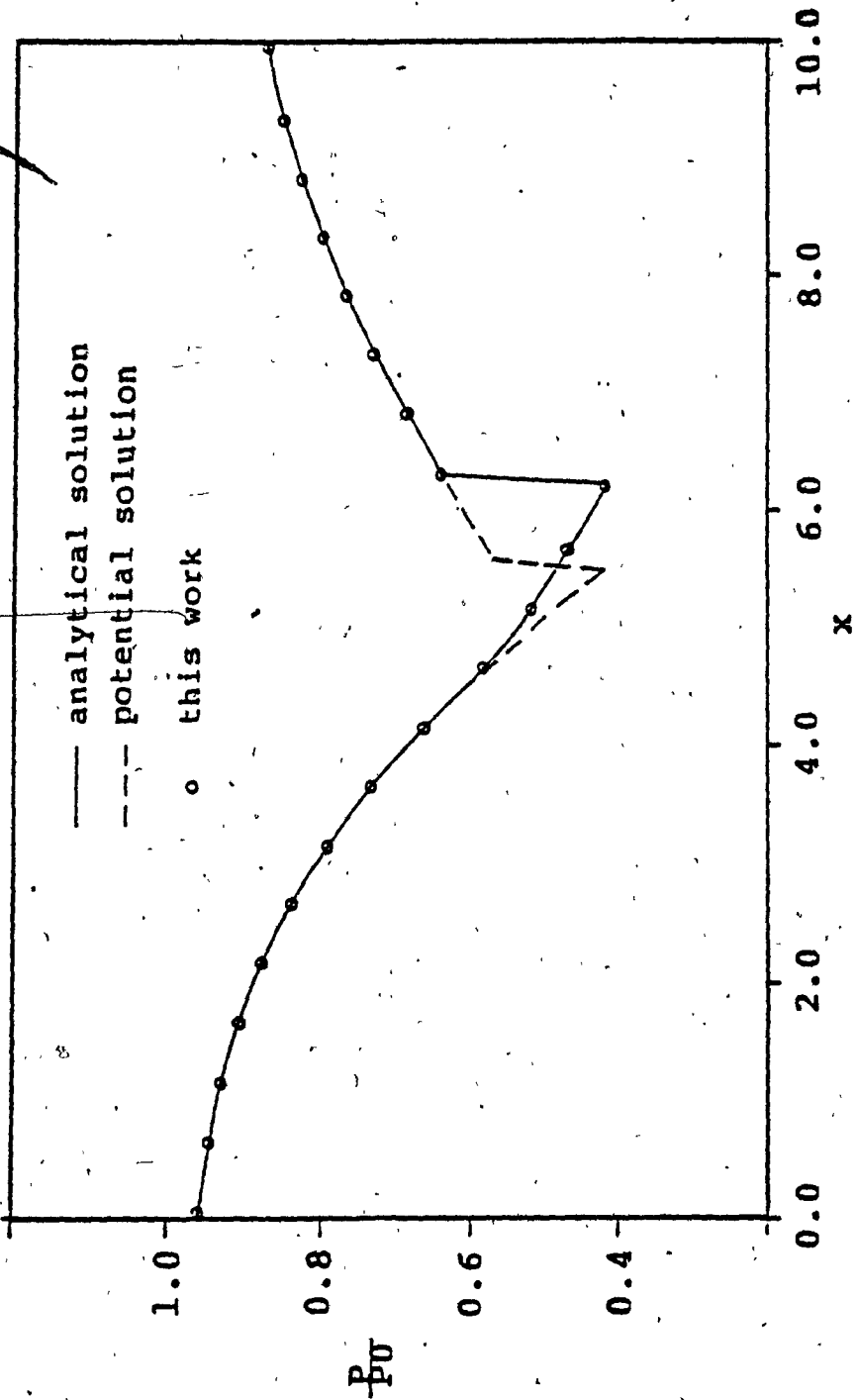


Fig. 6. Pressure distribution along the nozzle for transonic flow

REGION BOUNDARY EQUATION:

I	$y = 1.25 - 0.375 (x/8)^2$	$0 < x < 8$
II	$y = 0.50 + 0.375 [2 - (x/8)]^2$	$8 < x < 16$
III	$y = 0.50 + 0.125 [(x/8) - 2]^2$	$16 < x < 24$
IV	$y = 0.75 - 0.125 [(x/8) - 4]^2$	$24 < x < 32$

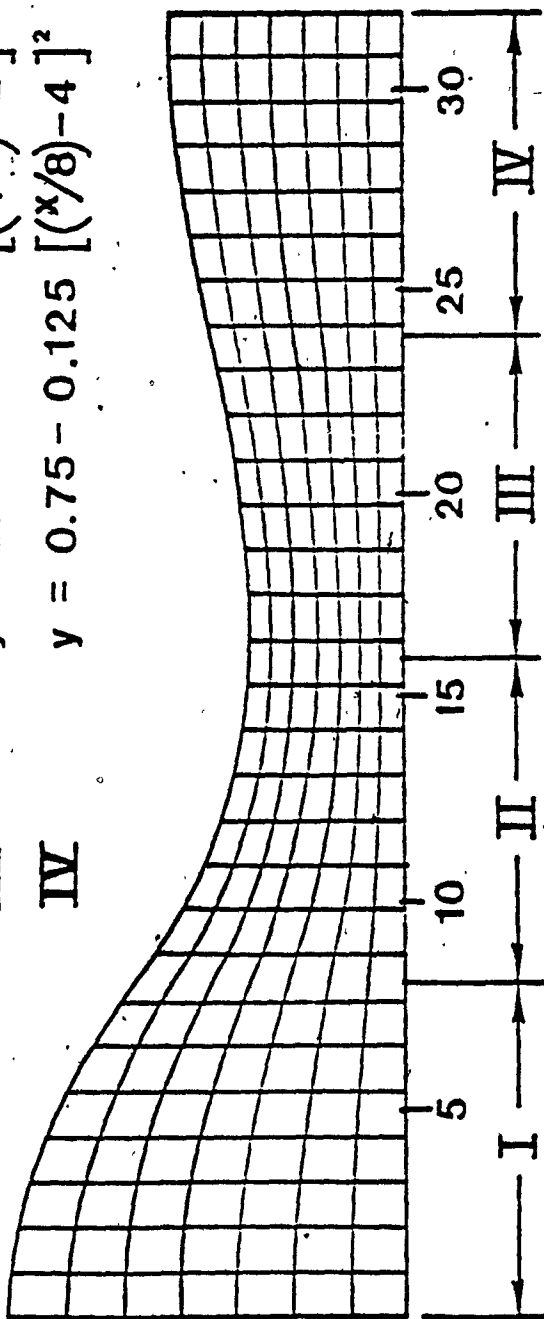


FIGURE 7. FINITE ELEMENT MESH FOR A TWO DIMENSIONAL NOZZLE FLOW

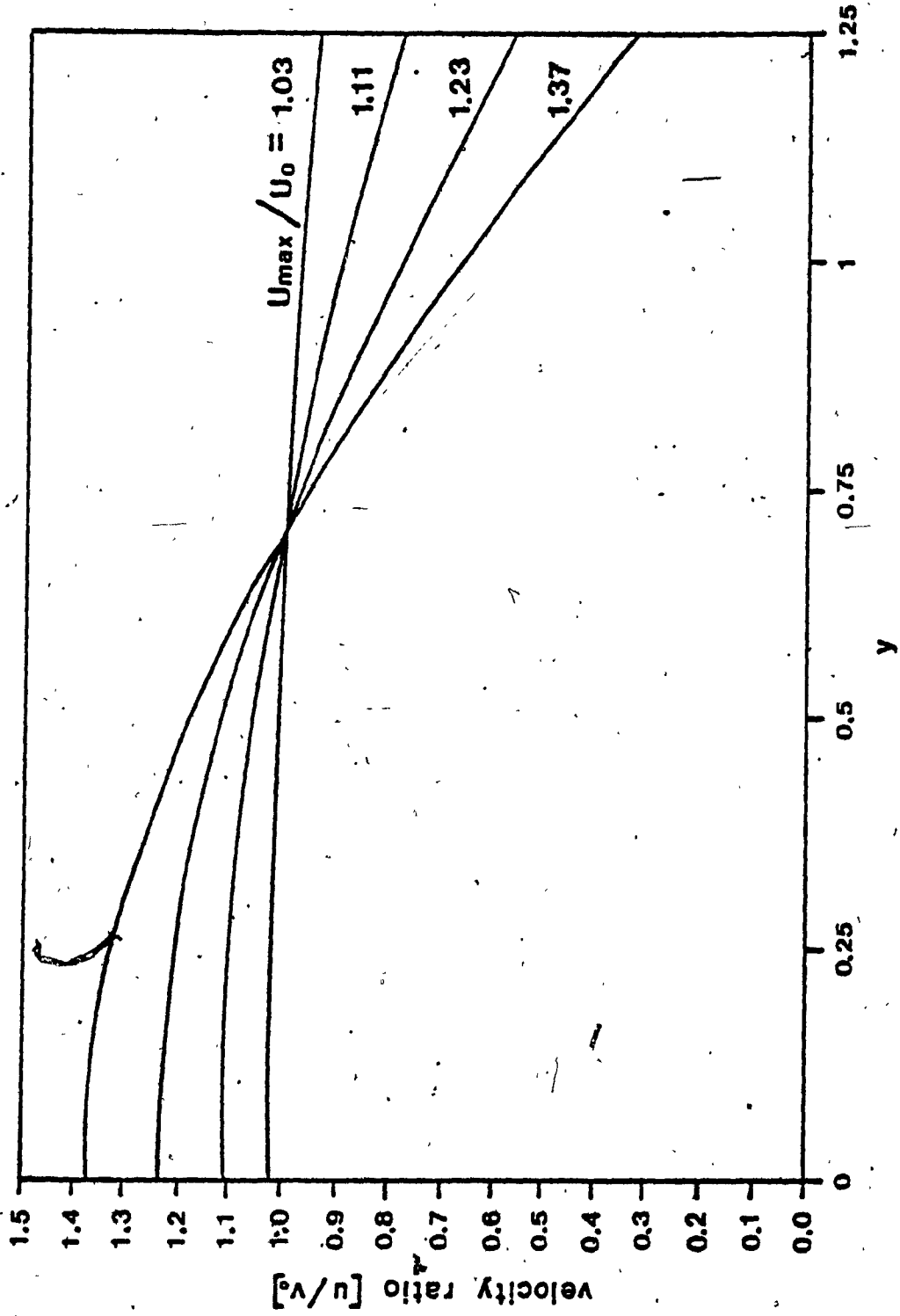


FIGURE 8. INLET VELOCITY RATIO PROFILES

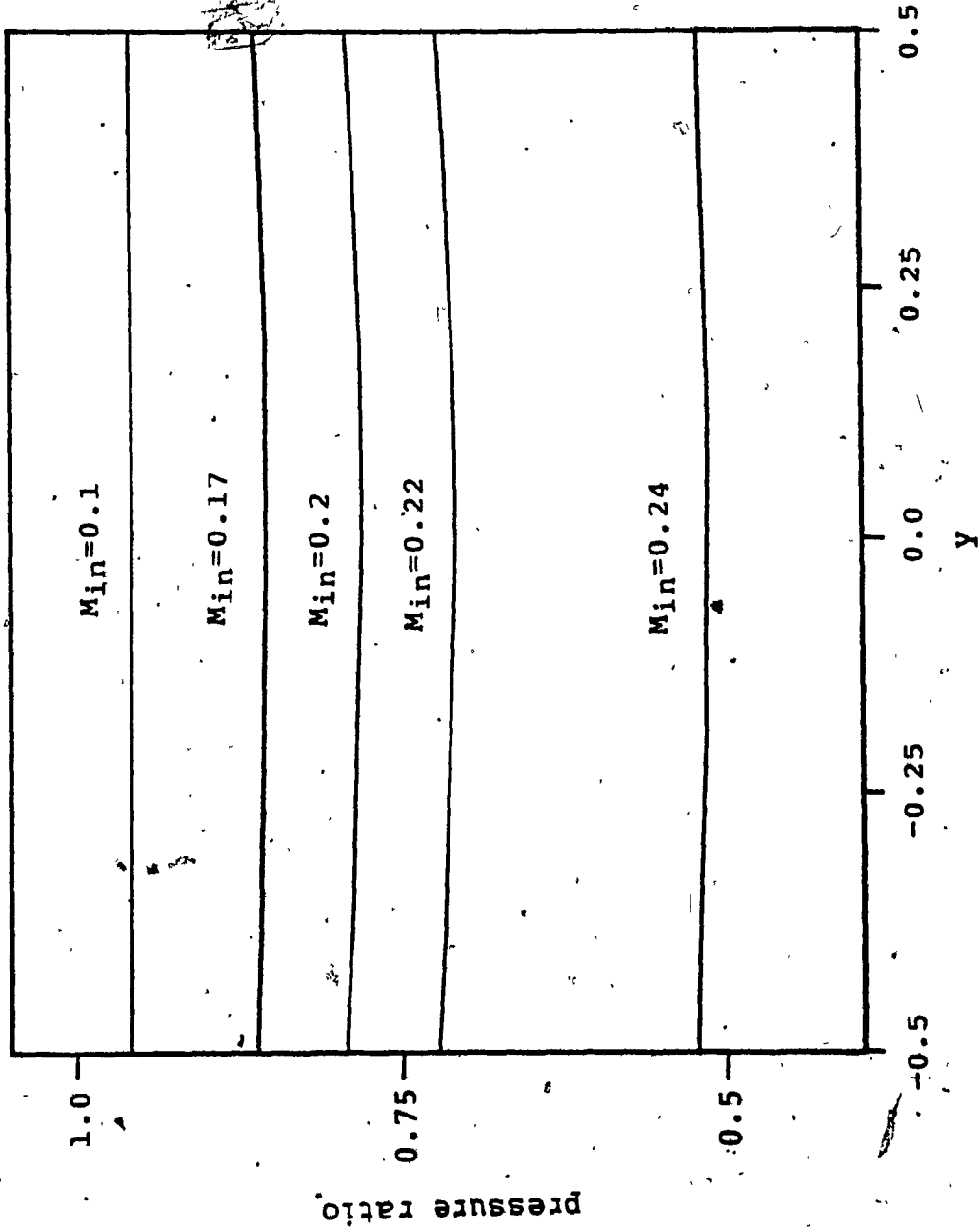


Fig. 9 Pressure profiles at the throat

--- isentropic stream lines
— stream line with rotation

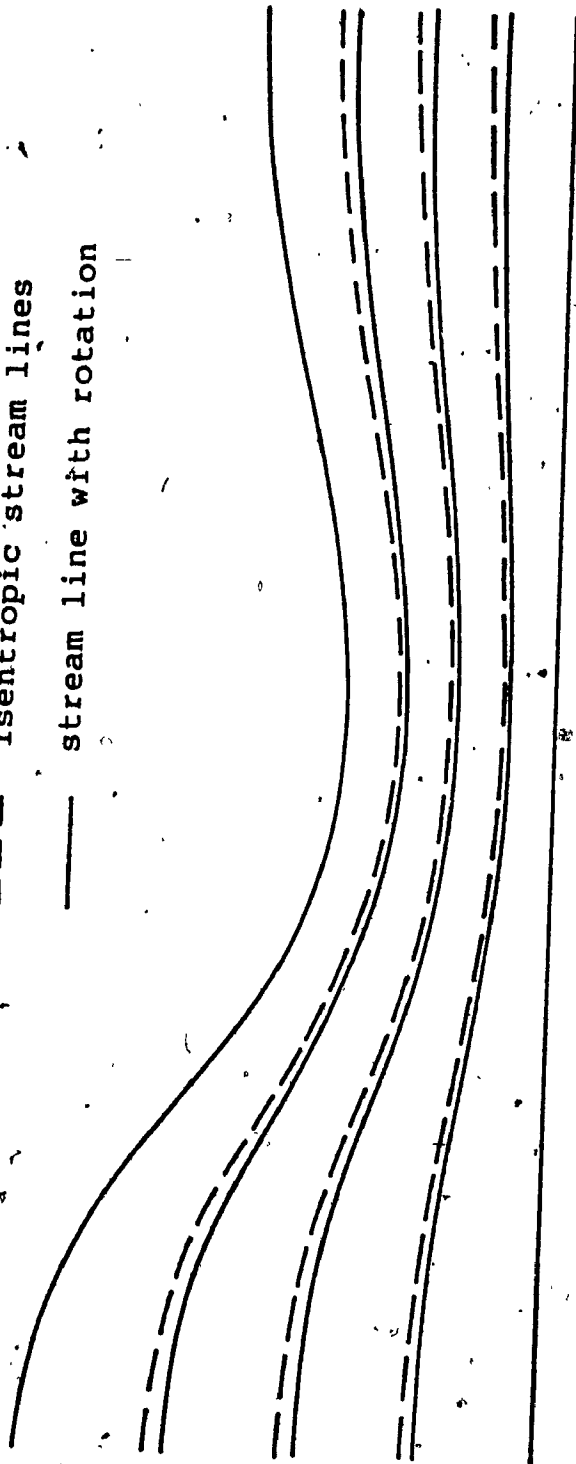


Fig. 10 Nozzle stream lines

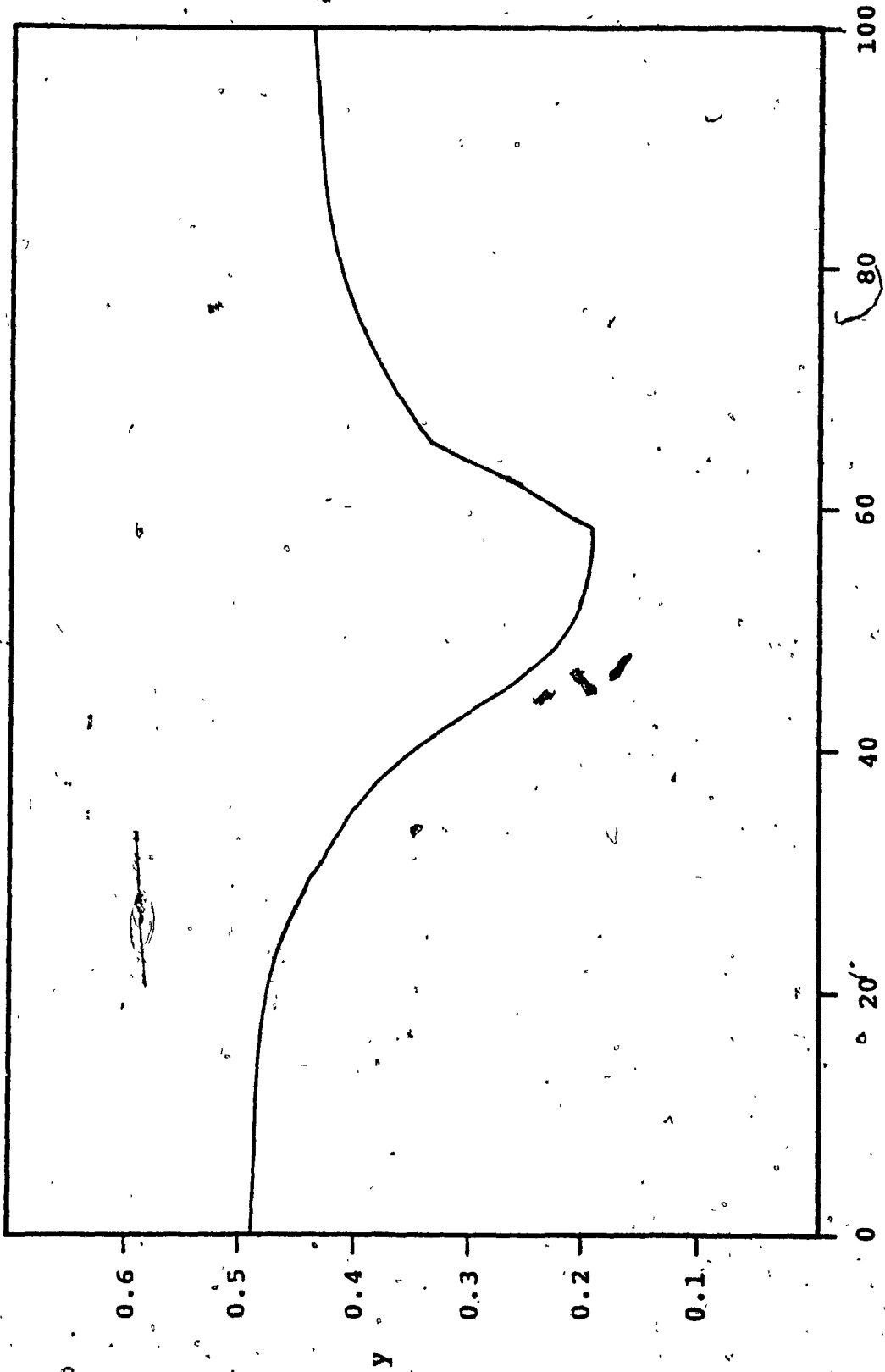


Fig. 11 Vorticity along the nozzle boundary

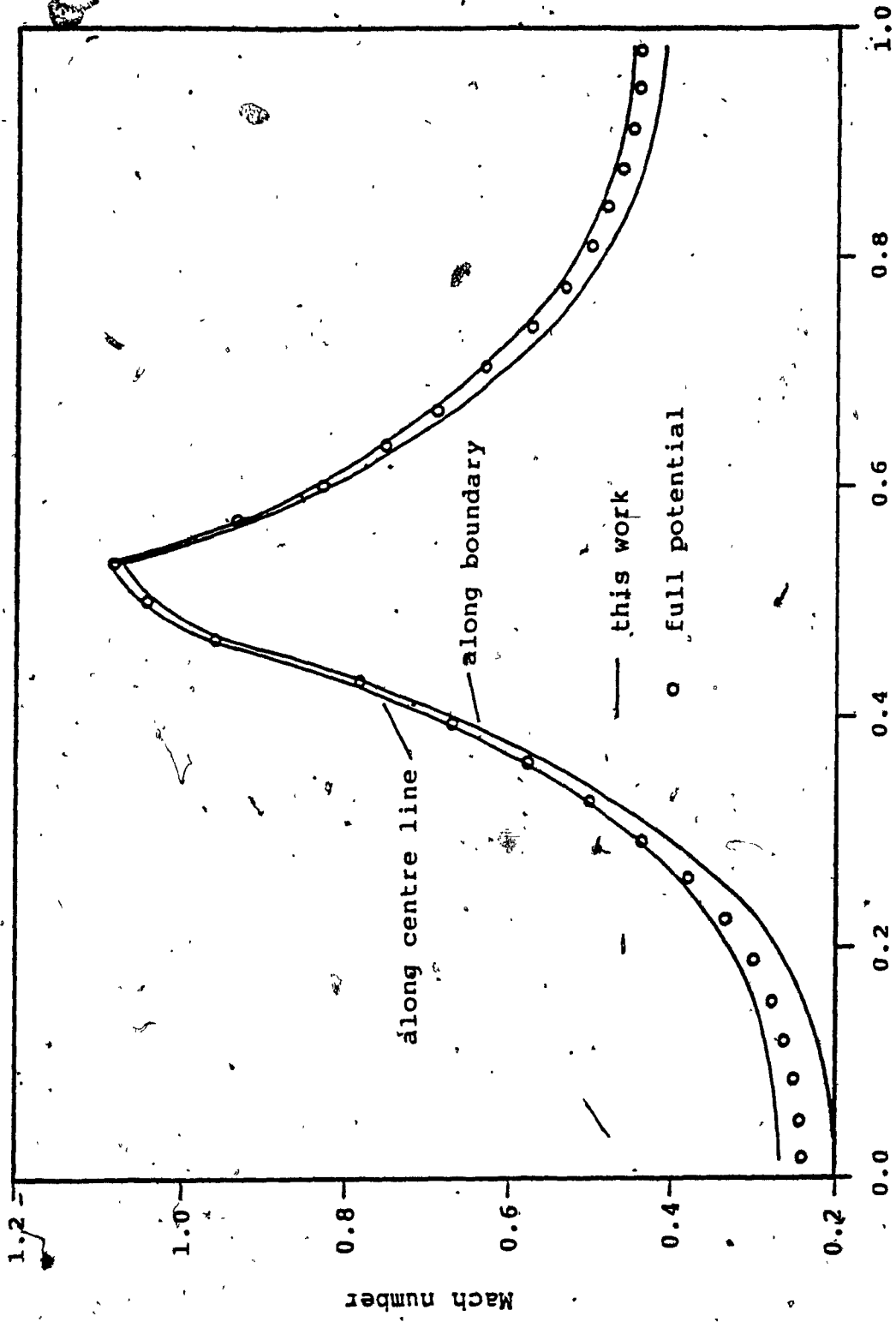


Fig. 12 Mach number along the nozzle

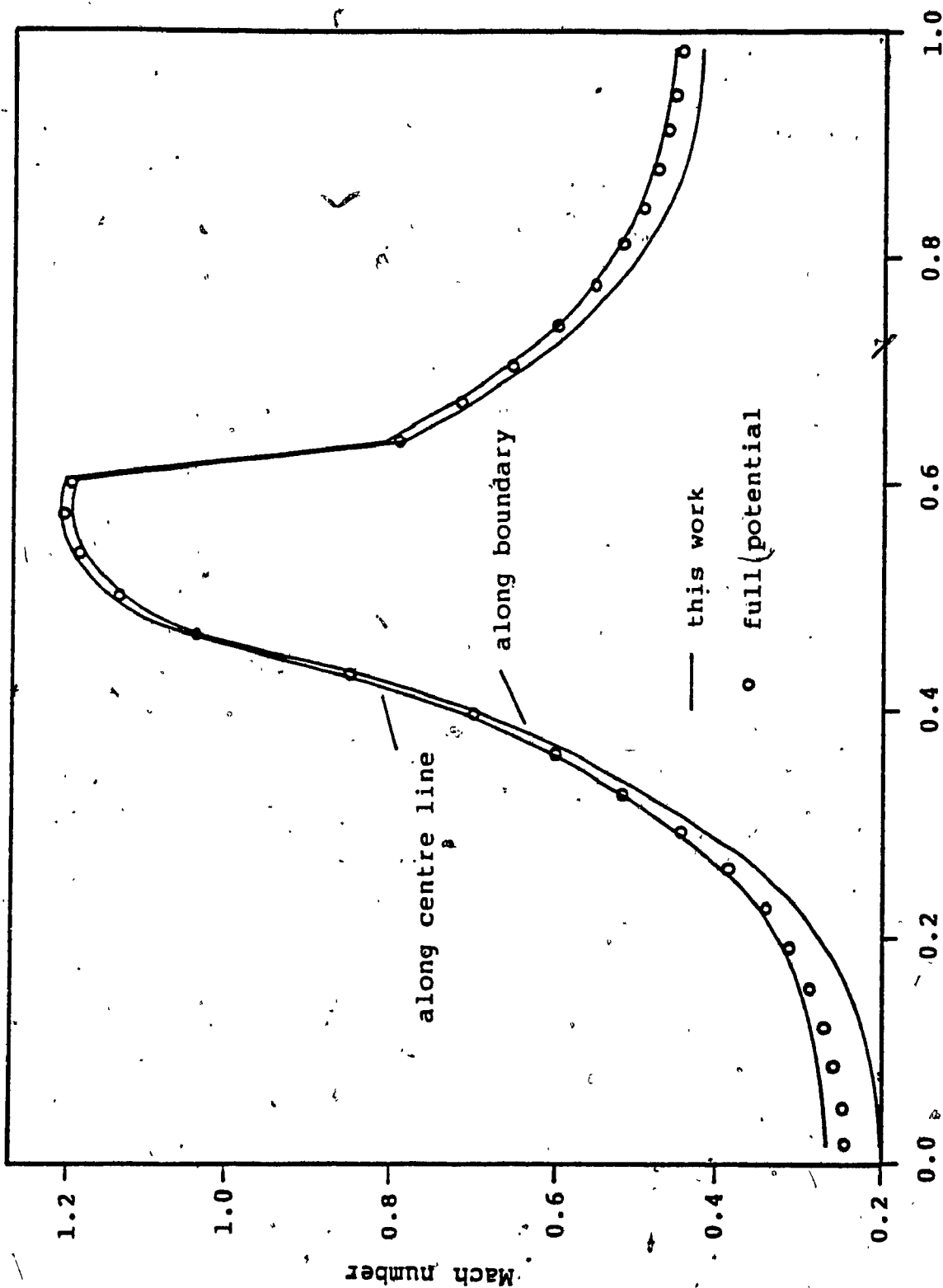


Fig. 13 Mach number along the nozzle

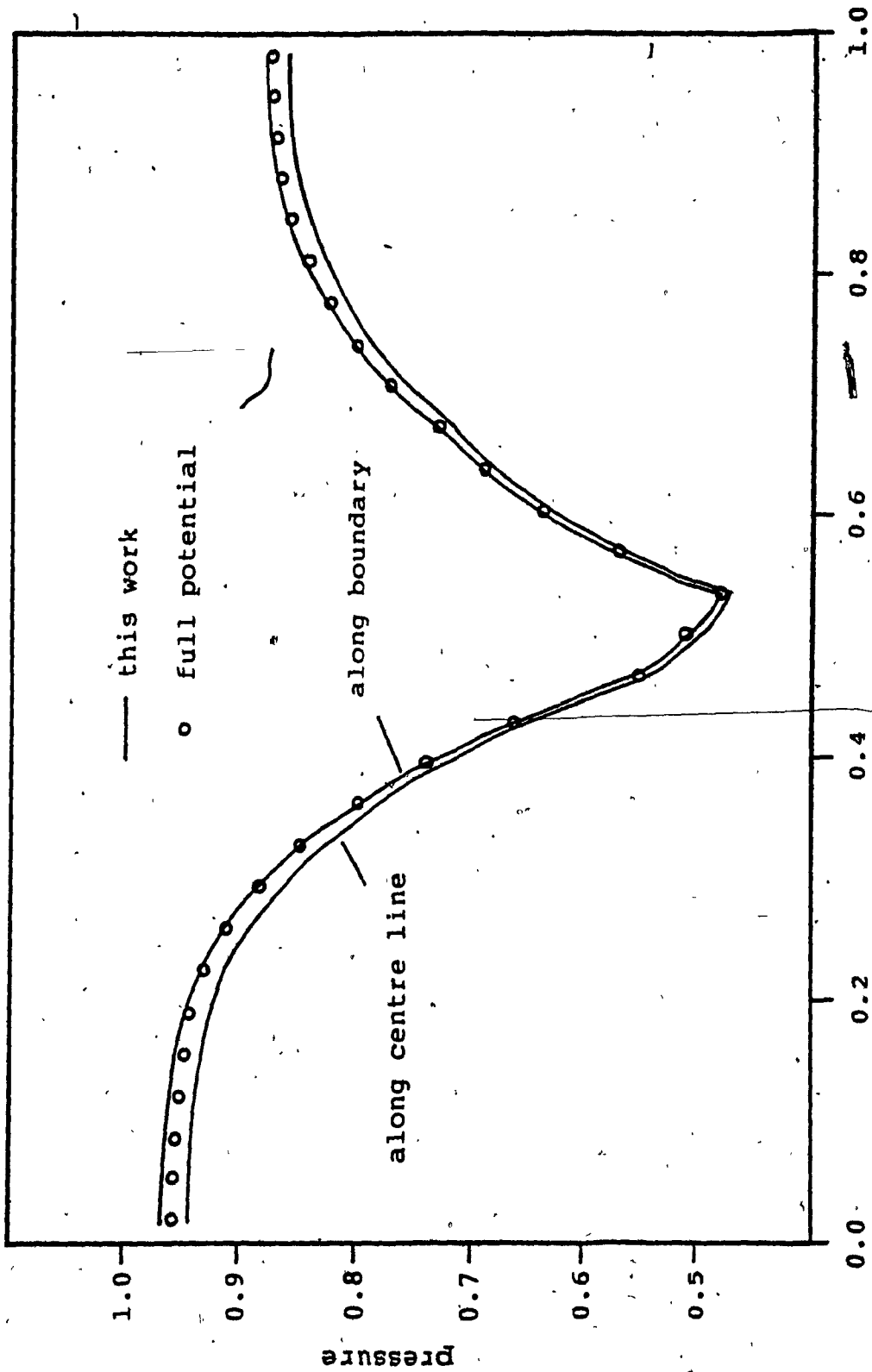


Fig. 14 Pressure distribution along the nozzle

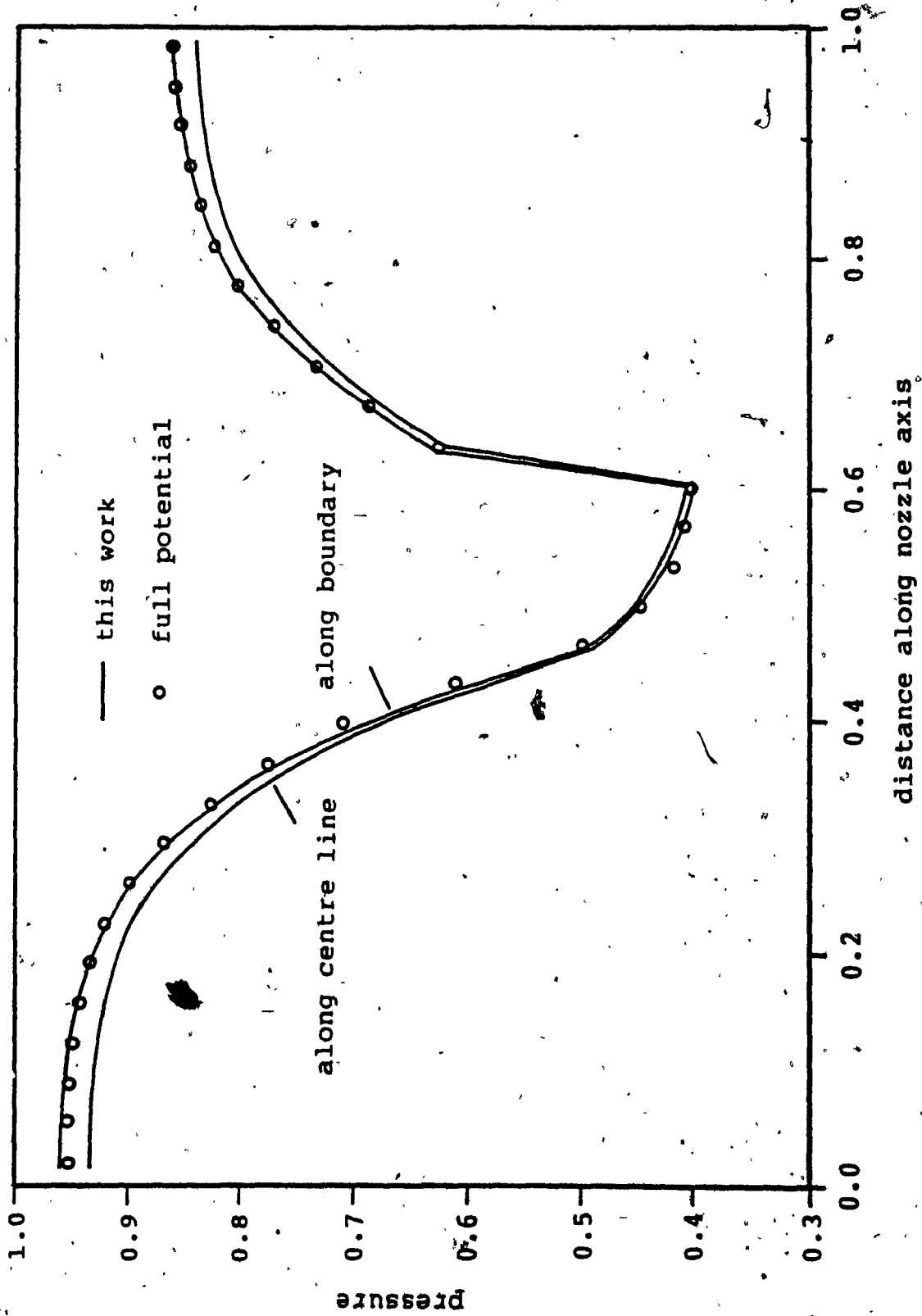


Fig. 15 Pressure distribution along the nozzle

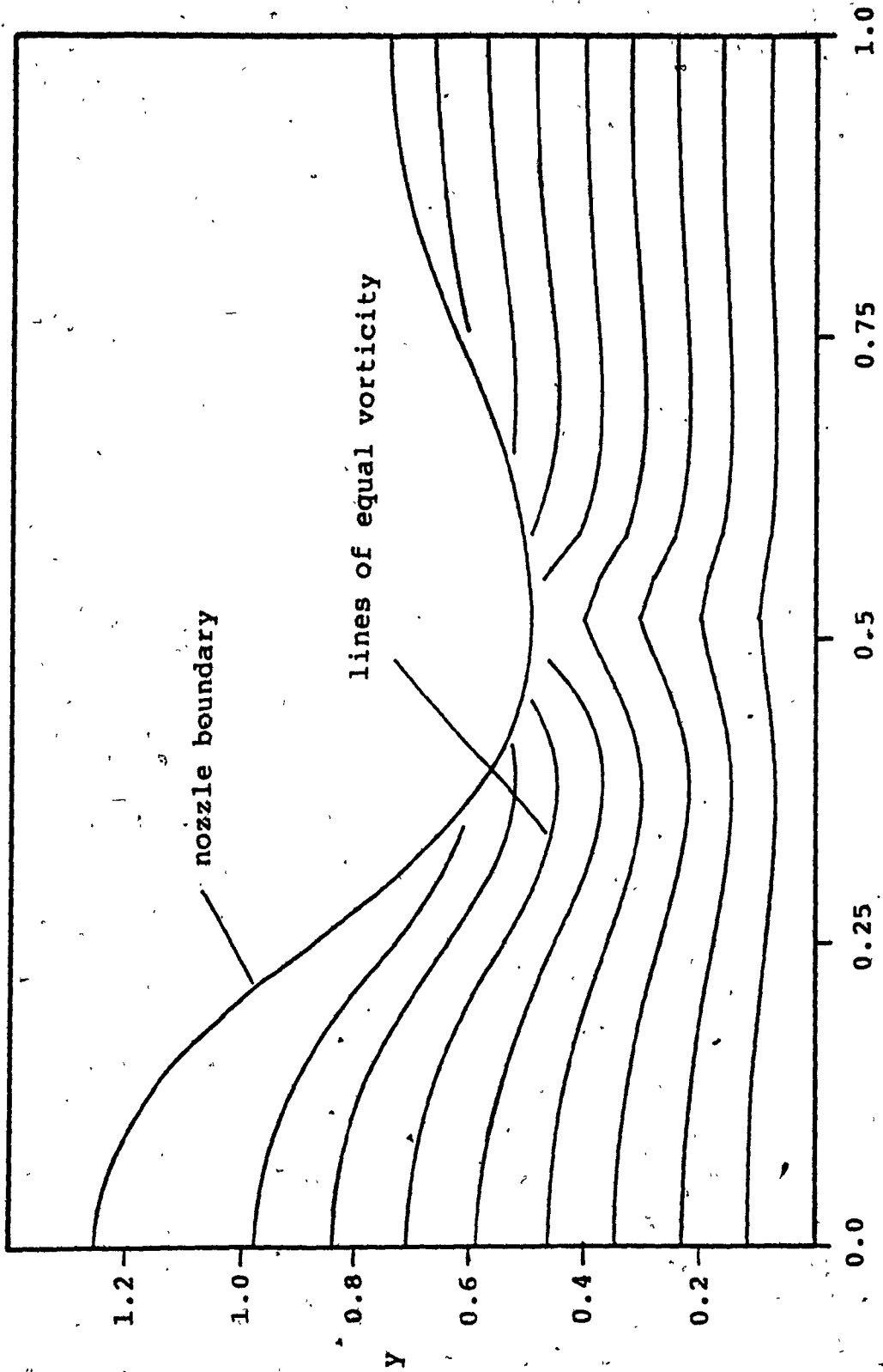


Fig. 16 Lines of equal vorticity

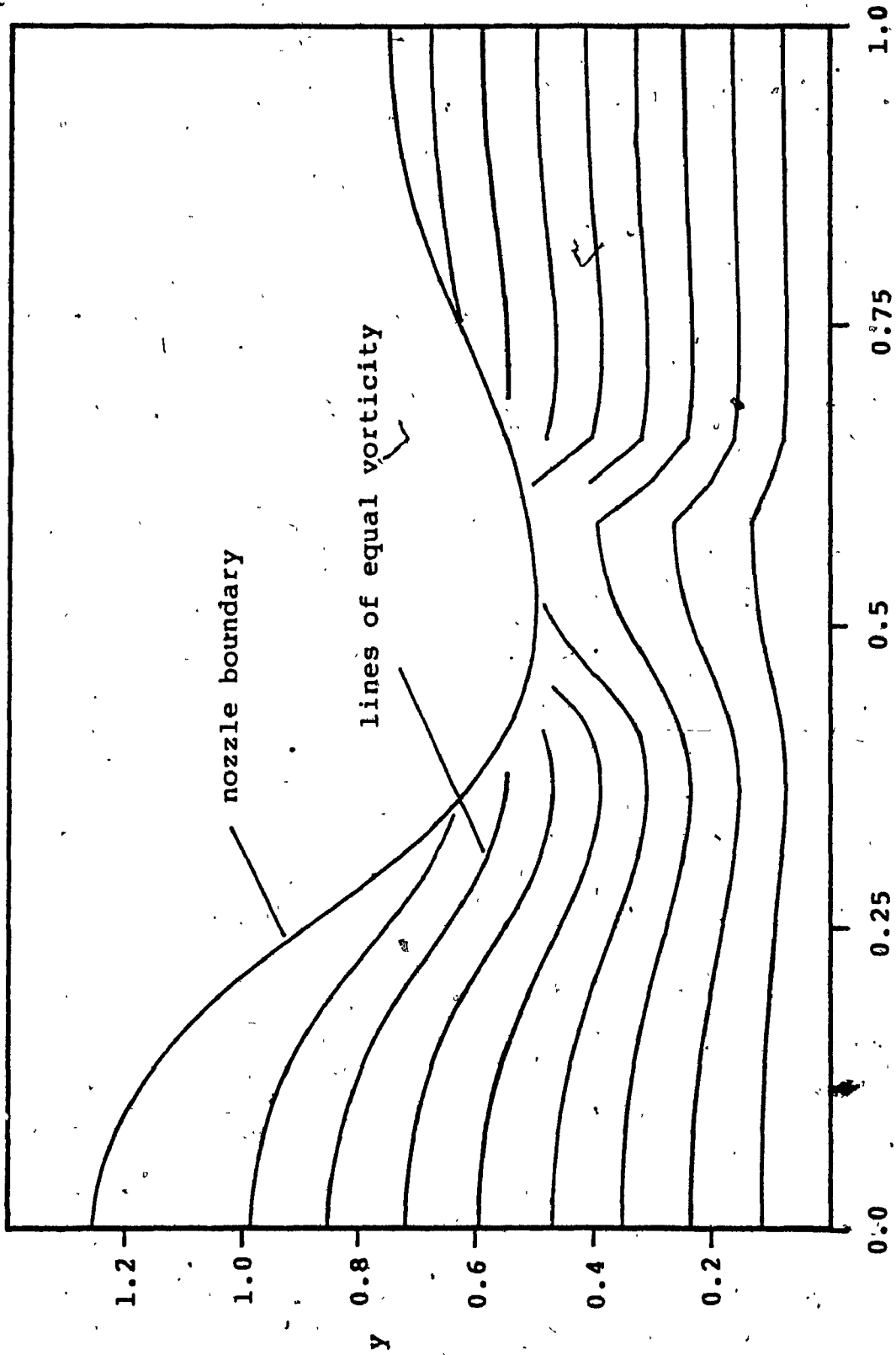


Fig. 17 Lines of equal vorticity

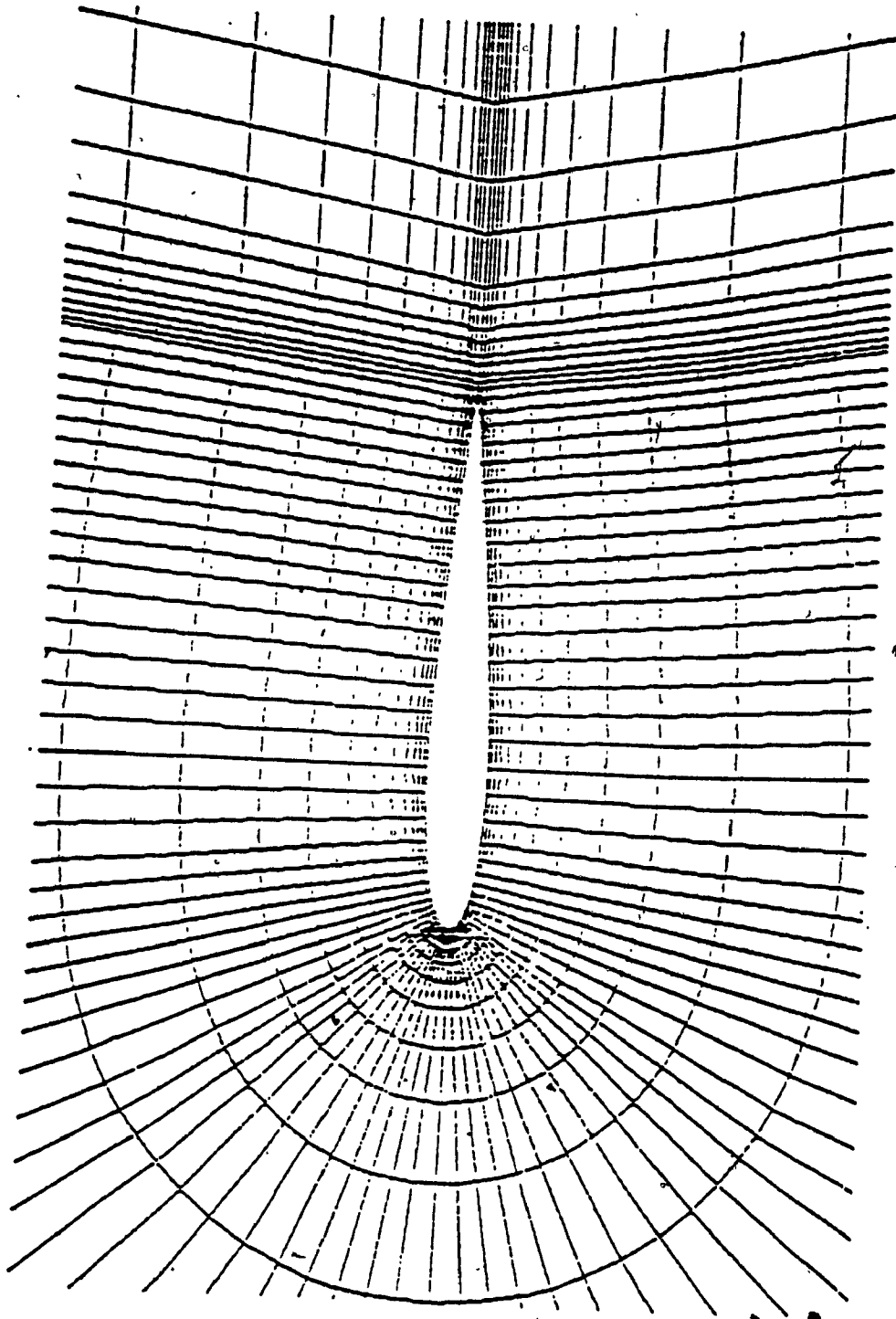


Fig. 18 Coarse grid for NACA-0012 airfoil

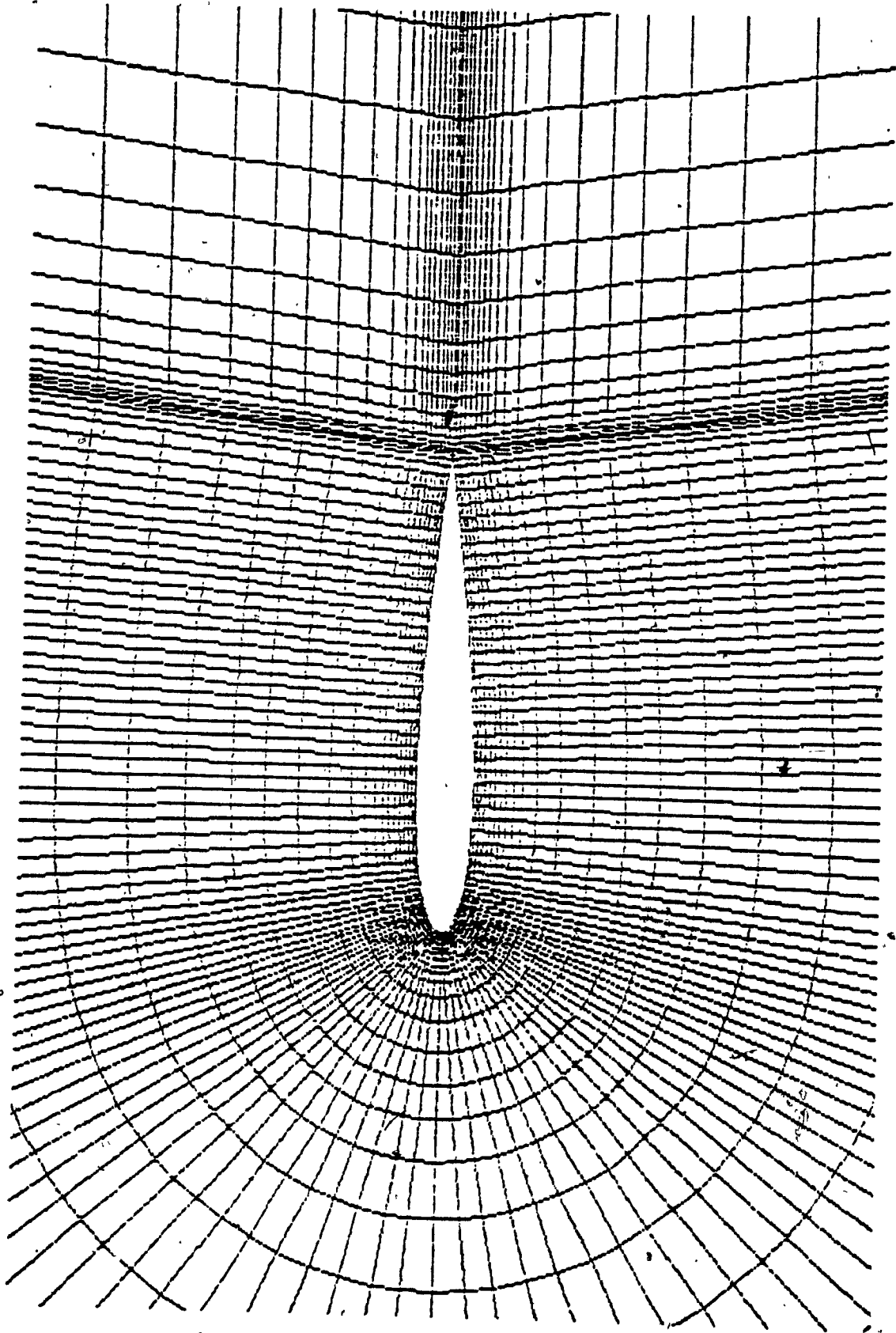


Fig. 19 Refined grid for NACA-0012 airfoil

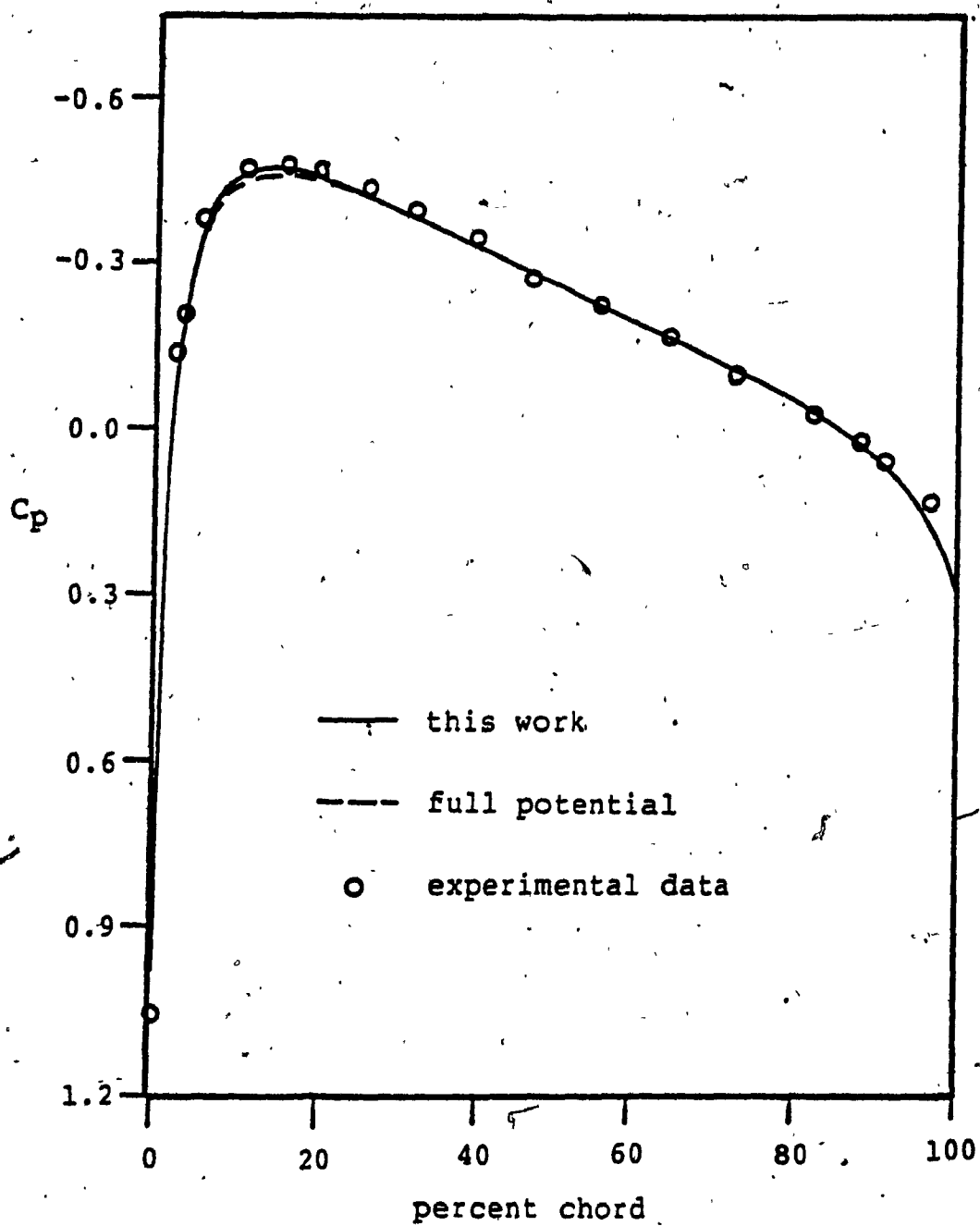


Fig. 20 Pressure coefficient on NACA-0012 airfoil

$$M_\infty = 0.5$$

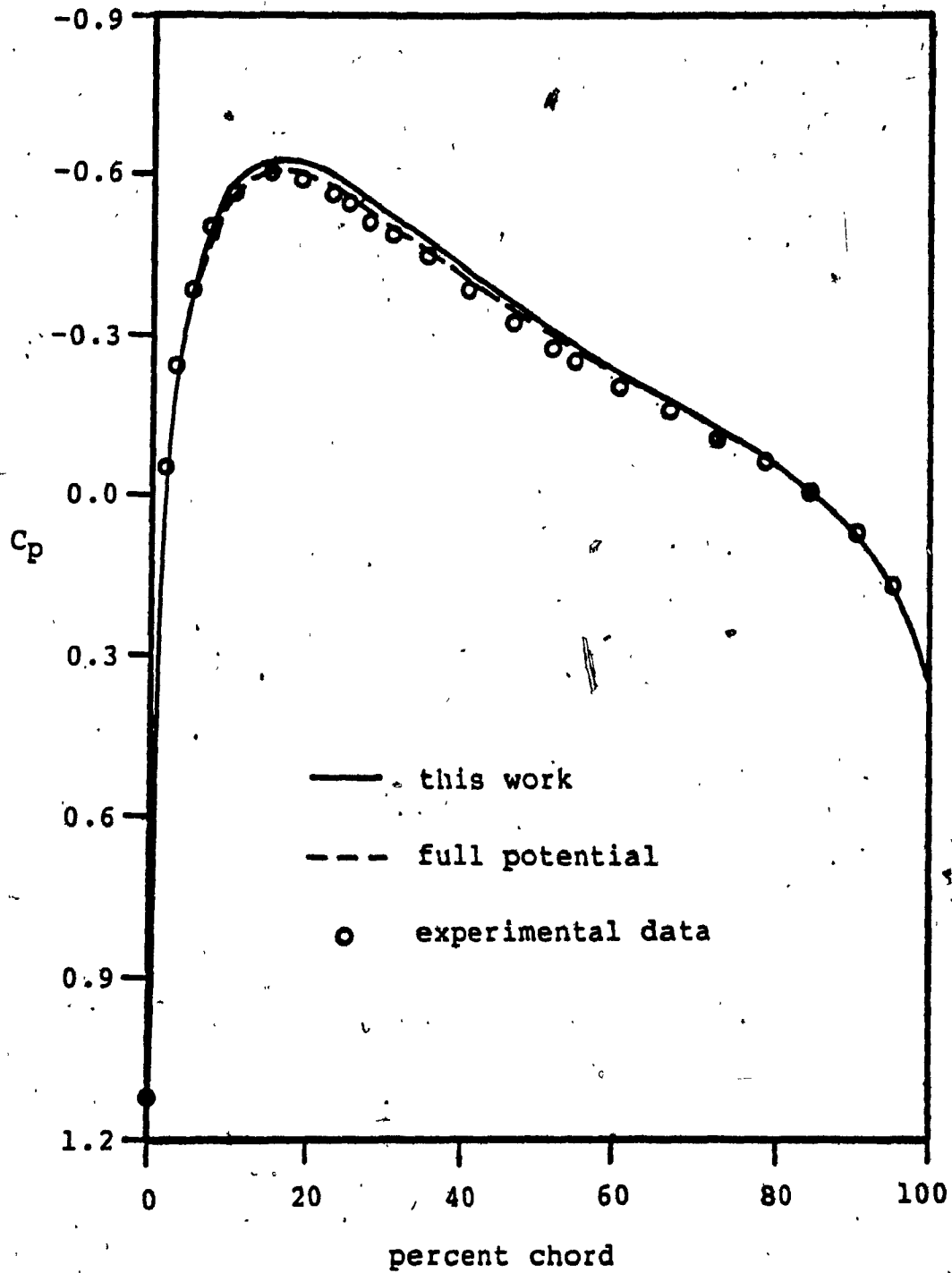


Fig. 21 Pressure coefficient on NACA-0012 airfoil

$$M_\infty = 0.703$$

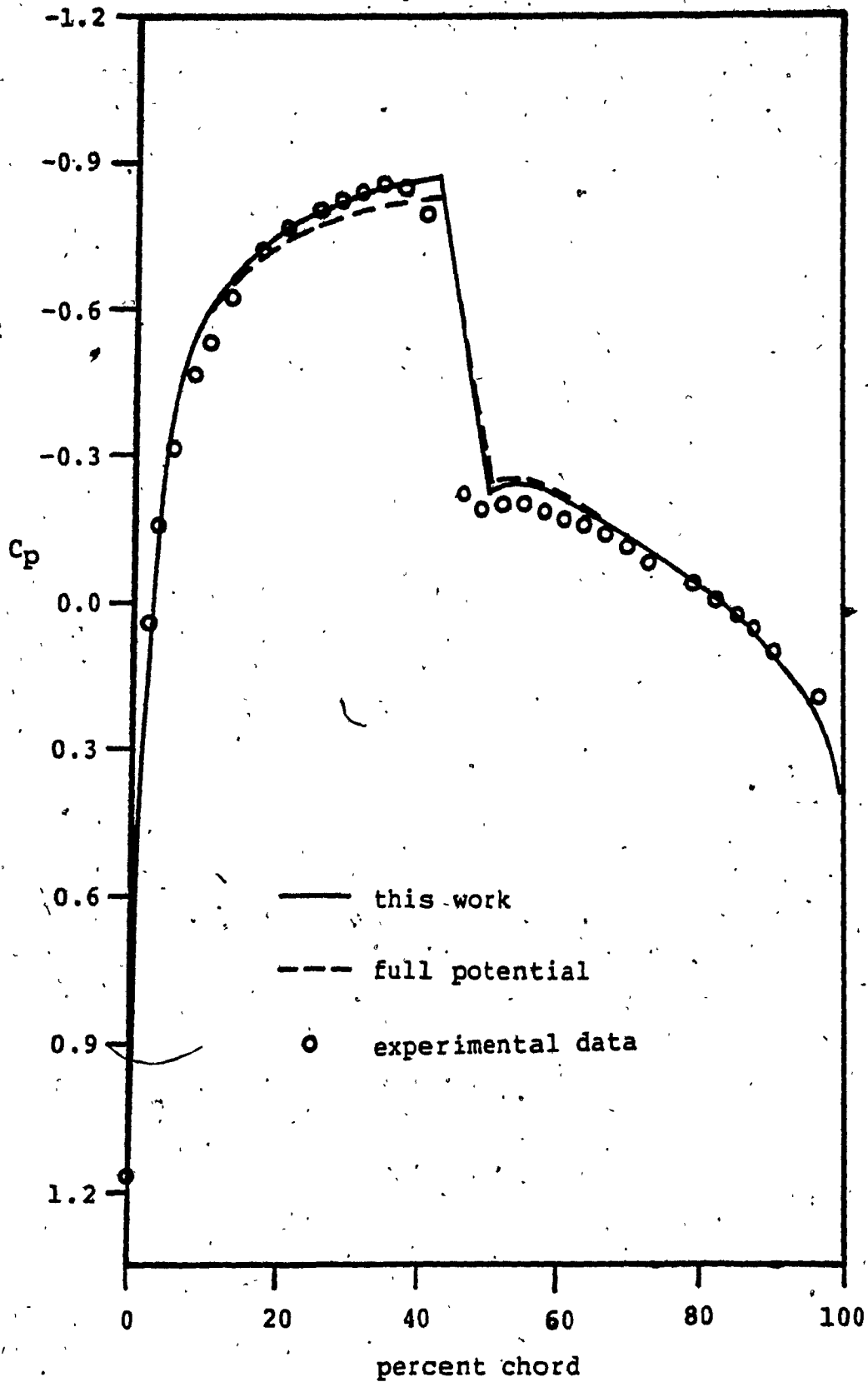


Fig. 22 Pressure coefficient on NACA-0012 airfoil

$$M_\infty = 0.803$$

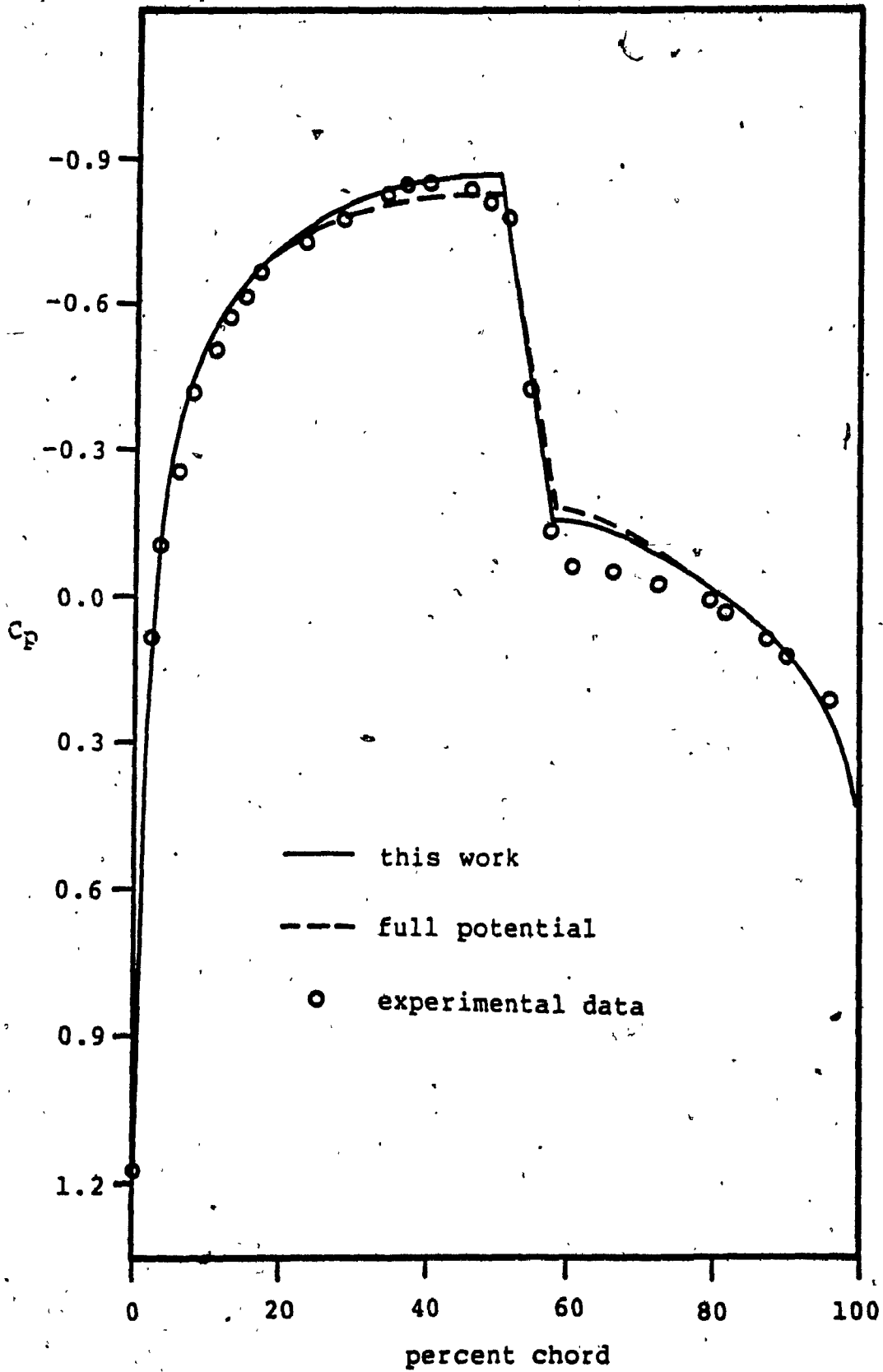


Fig. 23 Pressure coefficient on NACA-0012 airfoil

$M_\infty=0.829$

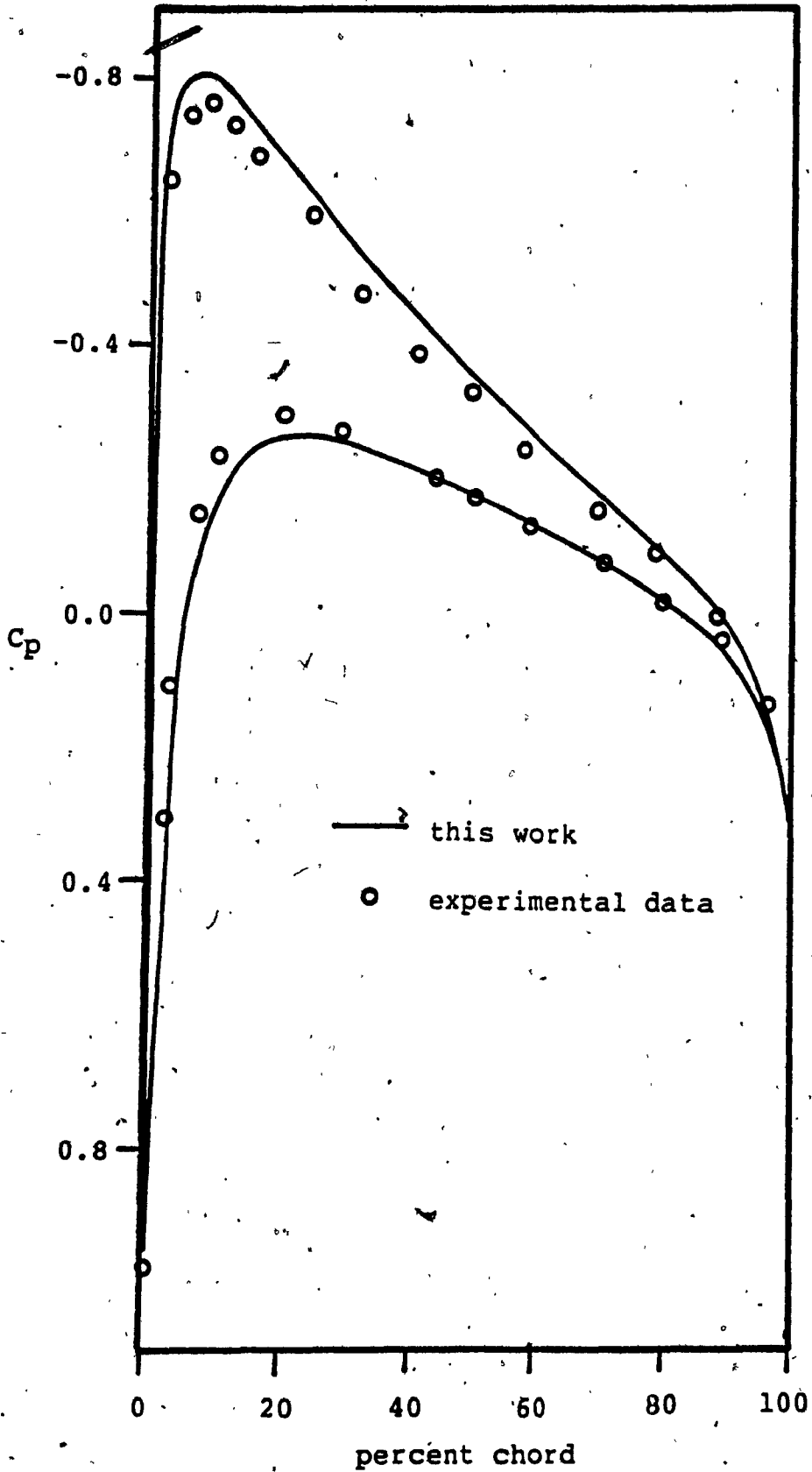


Fig. 24 Pressure coefficient on NACA-0012 airfoil

$\alpha=2.06$, $M_\infty=0.502$

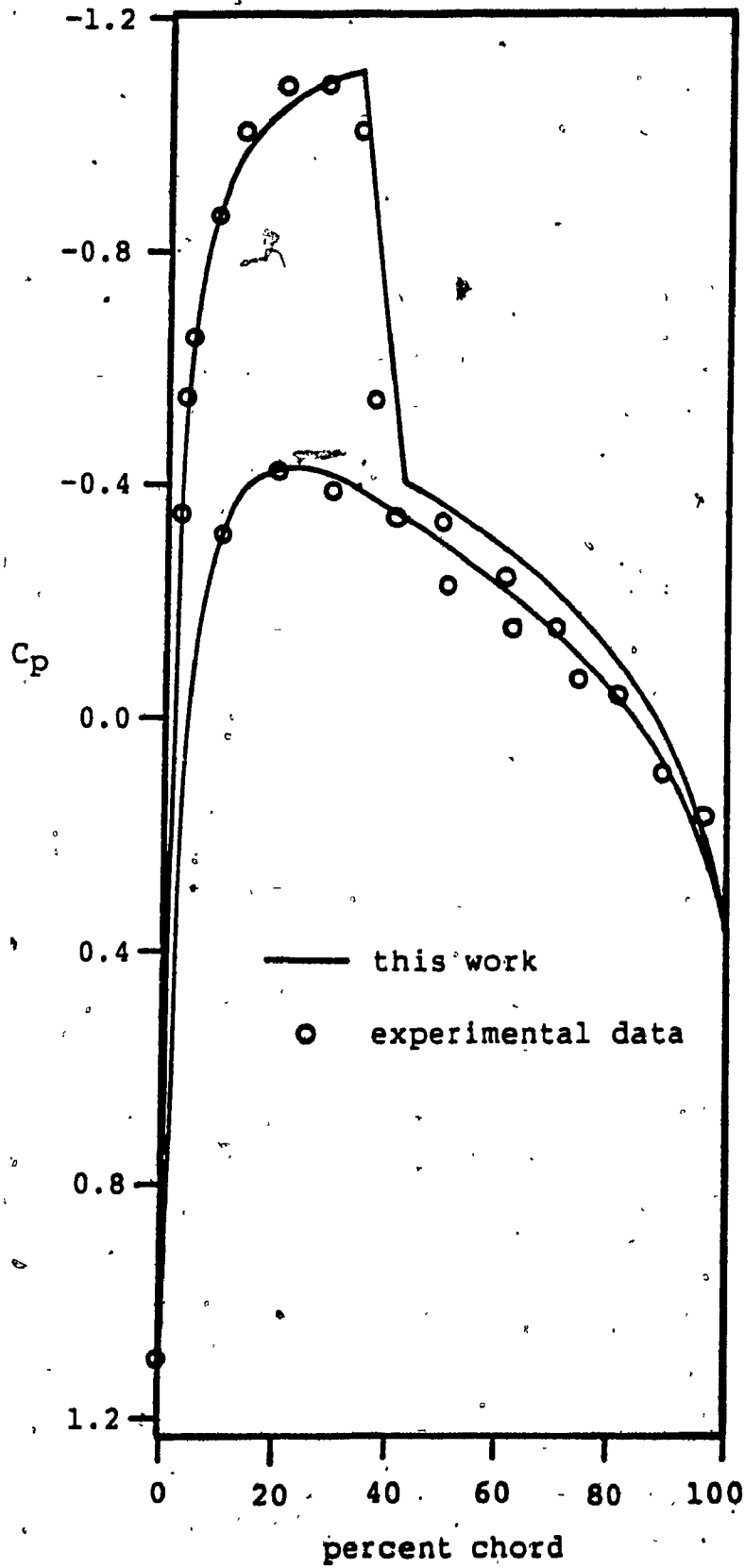


Fig. 25 Pressure coefficient on NACA-0012 airfoil

$\alpha=1.95$, $M_\infty=0.753$

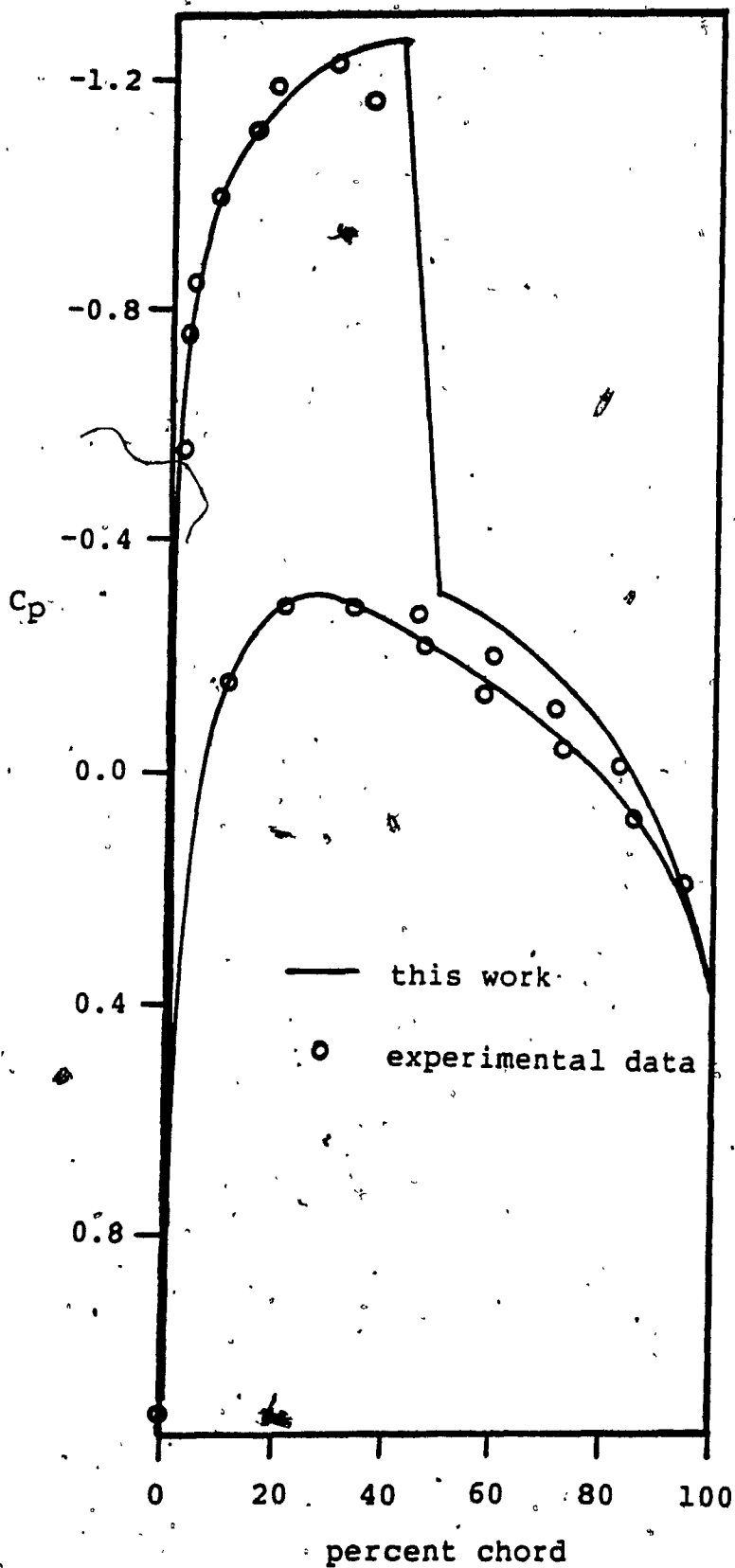


Fig. 26 Pressure coefficient on NACA-0012 airfoil

$\alpha=2.98$, $M_\infty=0.754$

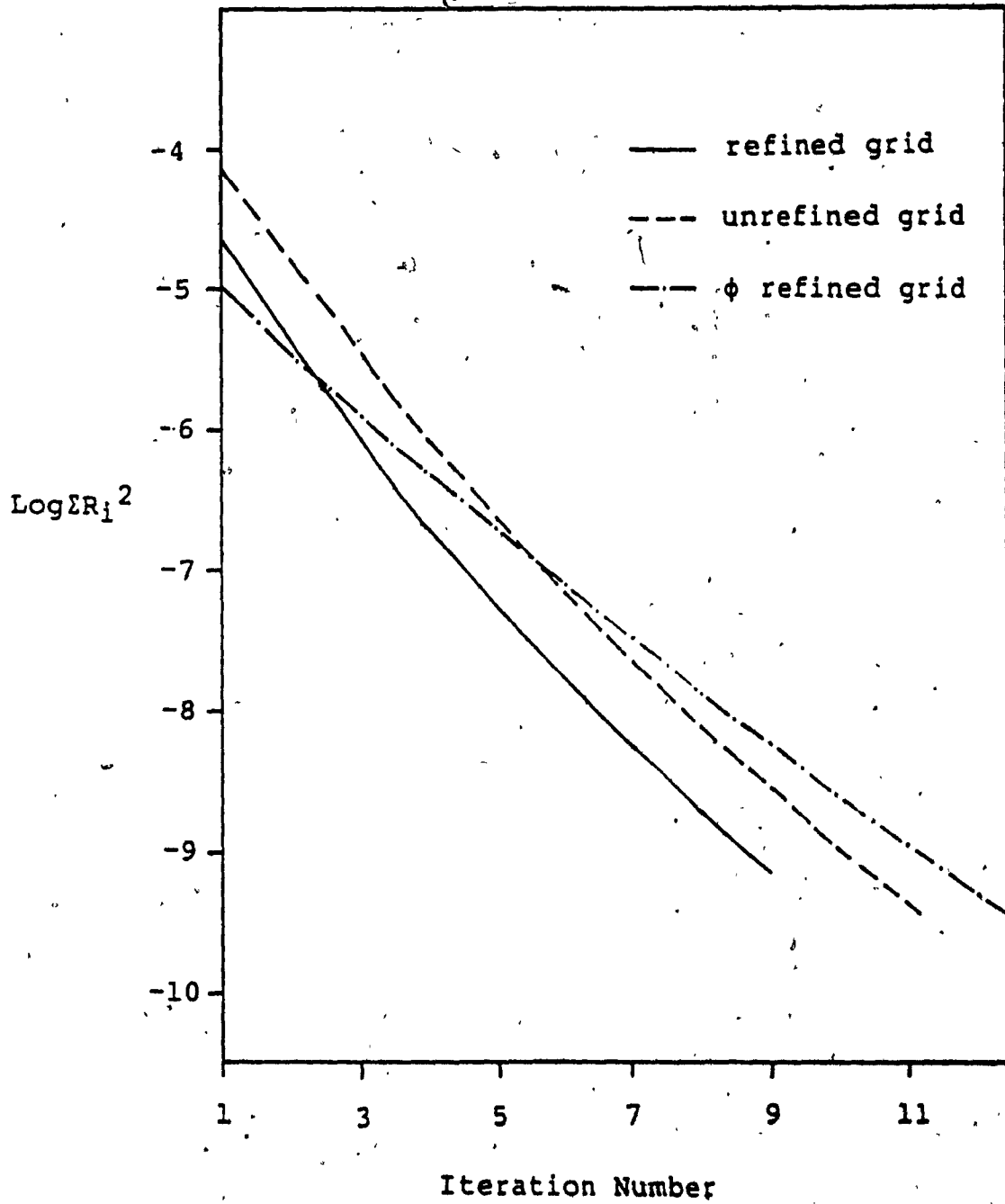


Fig. 27 Convergence history for NACA-0012 airfoil

$M_\infty = 0.703$

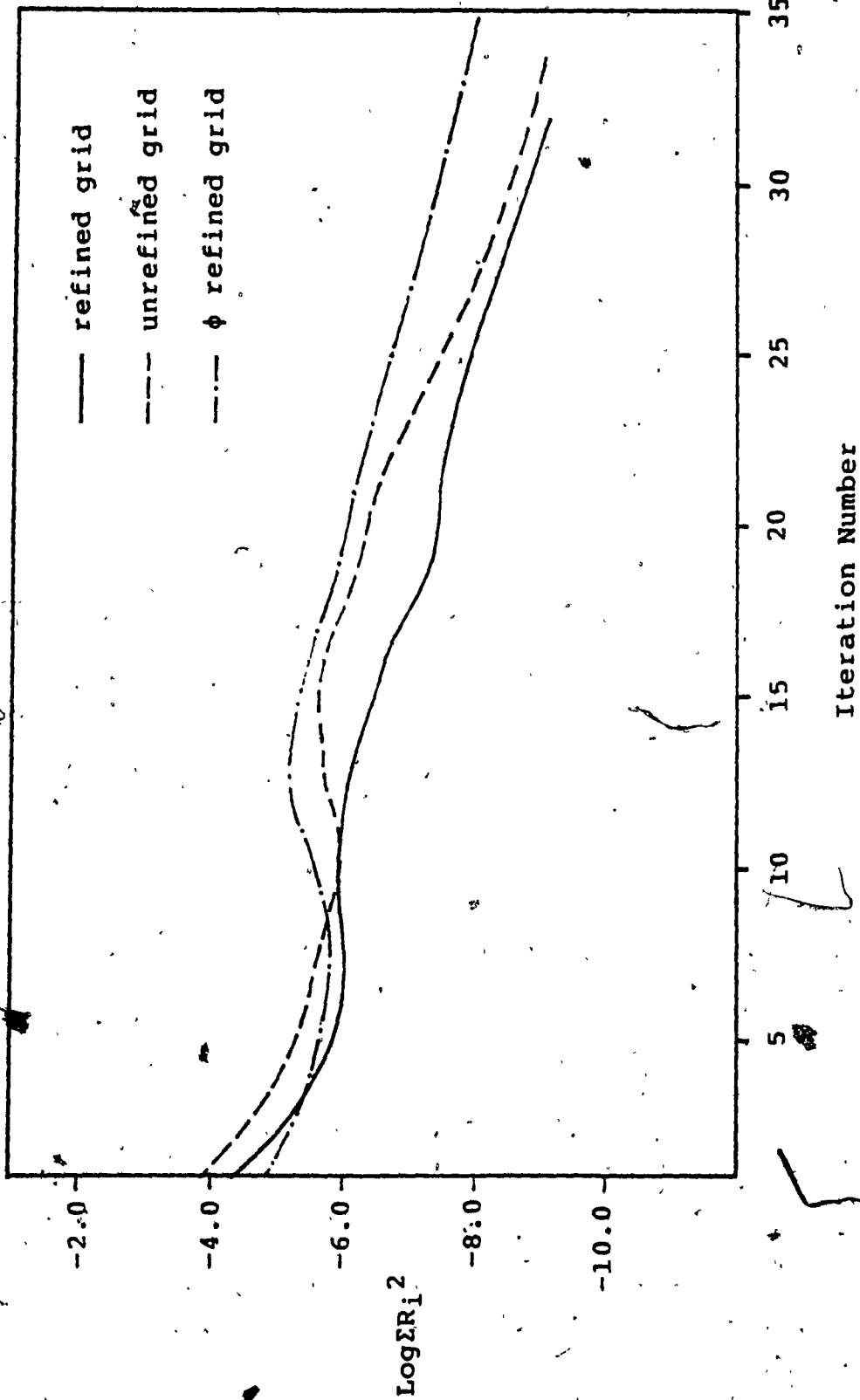


Fig. 28 Convergence history for NACA-0012 airfoil

$M_\infty = 0.803$

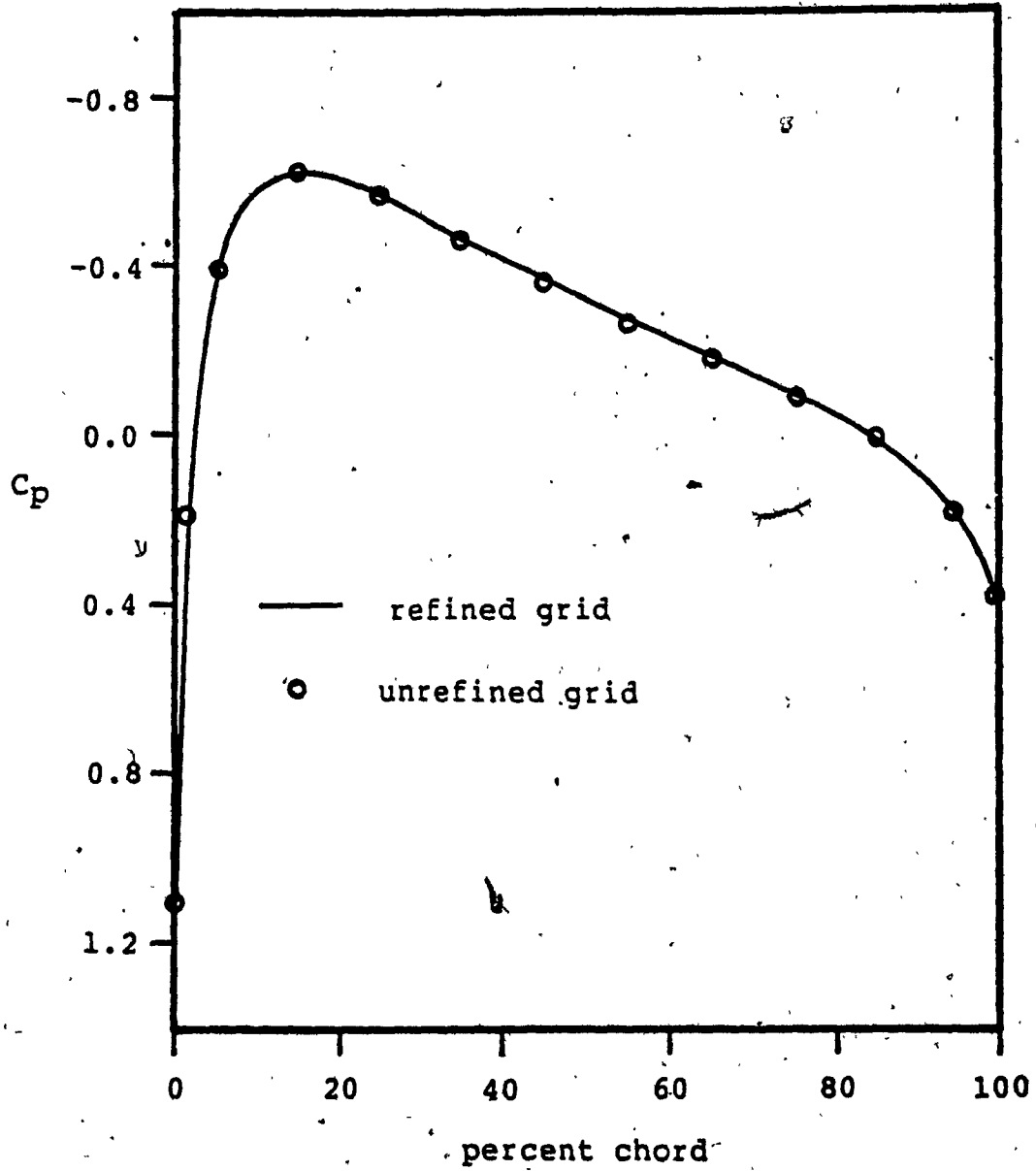


Fig. 29 C_p comparison for refined grid

$$M_\infty = 0.703$$

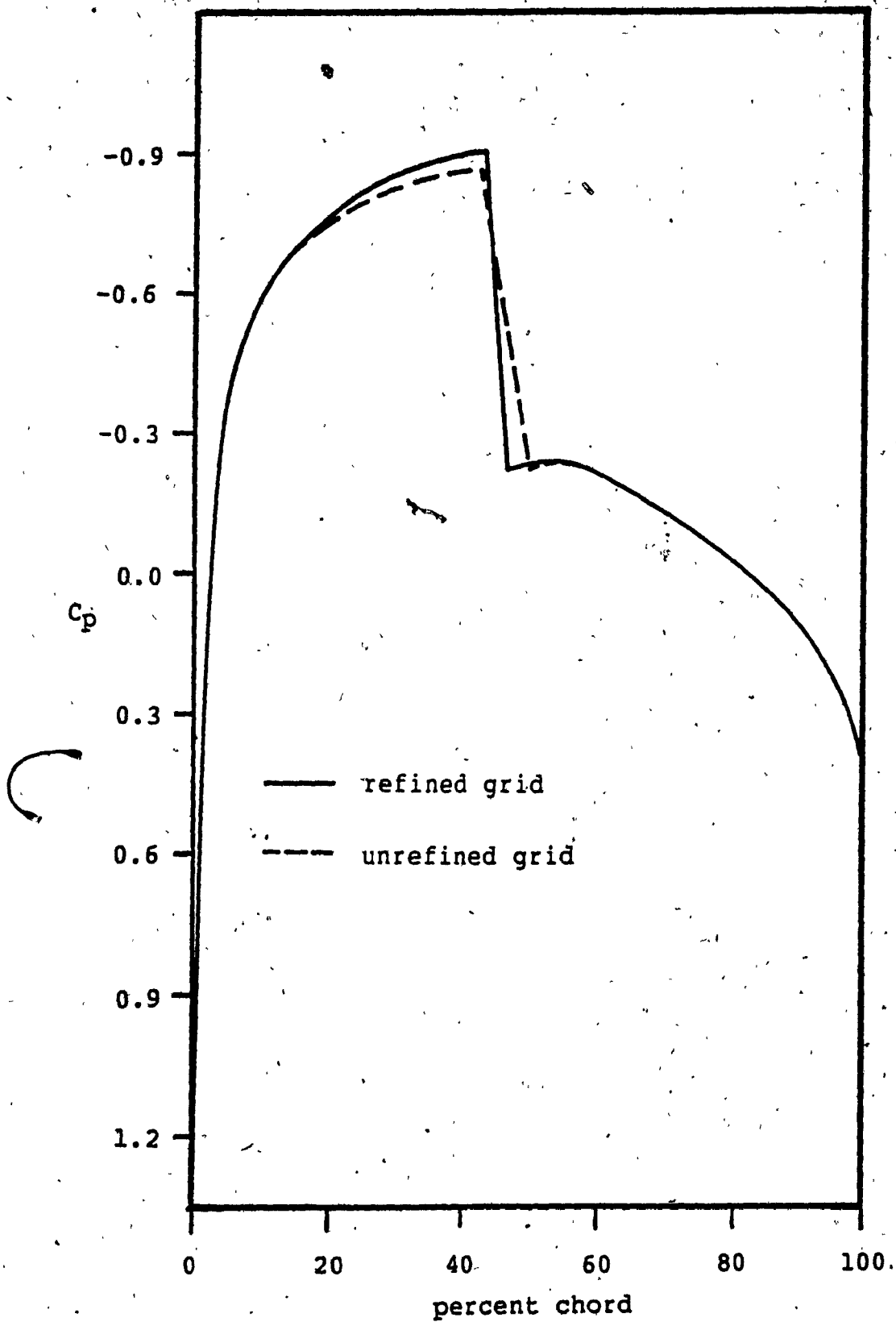


Fig. 30 C_p comparison for refined grid

$$M_\infty = 0.803$$